# MATHEMATICAL ANALYSIS OF SOIL TEMPERATURES IN AN ARID REGION

by

Kennith Earl Foster

---

A Dissertation Submitted to the Faculty of the

DEPARTMENT OF WATERSHED MANAGEMENT

In Partial Fulfillment of the Requirements
For the Degree of

DOCTOR OF PHILOSOPHY

In the Graduate College

THE UNIVERSITY OF ARIZONA

1 9 7 2

THE UNIVERSITY OF ARIZONA

GRADUATE COLLEGE

I hereby recommend that this dissertation prepared under my direction by Kennith E. Foster

entitled Mathematical Analysis of Soil Temperatures in an Arid Region

be accepted as fulfilling the dissertation requirement of the degree of Doctor of Philosophy

William R. Gardner — 11/10/71

Dissertation Director — Date

After inspection of the final copy of the dissertation, the following members of the Final Examination Committee concur in its approval and recommend its acceptance:*

| | |
|---|---|
| Martin N. Fogel | Nov. 10, 1971 |
| David B. Thorud | Nov. 10, 1971 |
| Hasan K. Qashu | Nov. 10, 1971 |
| K. E. Fye | Nov. 10, 1971 |
| Ahmed A. Evans | 12/8/71 |

*This approval and acceptance is contingent on the candidate's adequate performance and defense of this dissertation at the final oral examination. The inclusion of this sheet bound into the library copy of the dissertation is evidence of satisfactory performance at the final examination.

STATEMENT BY AUTHOR

This dissertation has been submitted in partial fulfillment of requirements for an advanced degree at The University of Arizona and is deposited in the University Library to be made available to borrowers under rules of the Library.

Brief quotations from this dissertation are allowable without special permission, provided that accurate acknowledgment of source is made. Requests for permission for extended quotation from or reproduction of this manuscript in whole or in part may be granted by the head of the major department or the Dean of the Graduate College when in his judgment the proposed use of the material is in the interests of scholarship. In all other instances, however, permission must be obtained from the author.

SIGNED: Kenneth E. Foster

ACKNOWLEDGMENTS

I am greatly indebted to Dr. R. E. Fye, Cotton Insects Biological Control Laboratory, USDA, Tucson, Arizona, who made available all field equipment necessary to collect the field data.

I also wish to express my appreciation to Dr. William D. Sellers for the patient guidance and encouragement given me during this study.

TABLE OF CONTENTS

TABLE OF CONTENTS--Continued

LIST OF TABLES

LIST OF TABLES--Continued

LIST OF ILLUSTRATIONS

ABSTRACT

A mathematical model study was made to compare simulated soil temperature variations with a field situation. The study involved the use of two plots, one of which was cleared of all vegetation and the other left in its natural vegetative state. Each plot was watered at the beginning of three different trial periods and as drying occurred, the following atmospheric parameters were measured on an hourly basis: incoming solar radiation, air temperature, relative humidity, cloud cover, and wind speed. The above parameters provided input for solution of the energy budget equation to determine soil surface temperature variation. Using the soil surface temperature variation as an upper boundary condition, and assuming heat movement by conduction, the temperature at 5 cm increments down to 70 cm in the soil was calculated.

The two plots provided model testing for a bare soil surface and also for a soil surface beneath a 30 percent and a 40 percent plant cover. Actual and calculated temperature difference was in most cases less than 2°F.

The mathematical model is applicable to any area where the above parameters may be monitored.

# INTRODUCTION

Soil temperature is one of the most important factors controlling plant growth and development. While measurements of soil temperature are being carried out on a large scale and under a great variety of conditions, the physical mechanism of the main energetic processes (the exchange of heat between the soil surface and the deeper layers of the soil or air above, evaporation from the surface, etc.) remain largely unexplored.

## Statement of the Problem

In problems which concern the heat regime of the soil, there is a contrast between the stress laid on the measurement of soil temperature, and the interpretation of the mechanism of heat transfer and the role of the heat balance in the energetic state of the soil. Many efforts have been made to determine soil temperature profiles. Field methods exist for determining temperature profiles using thermocouples placed beneath the soil surface, but natural field conditions must be altered to install them. Soil temperature records have been analyzed mathematically assuming a homogeneous soil profile with a periodic sinusoidal temperature variation at the soil surface. A need exists for a mathematical model to determine soil temperature profiles from atmospheric data. Hence subsurface soil temperatures could be analyzed in their natural state, and the temperature variation with time at the surface will be known and not assumed.

## Purpose of the Investigation

The purpose of the investigation was to compare the soil profile temperature variation simulated by a mathematical model to that of a field situation. Various atmospheric parameters were measured or estimated. They include: 1) total incoming solar radiation, 2) air temperature, 3) relative humidity, 4) cloud cover, 5) wind speed, 6) exchange coefficient for convective heat transfer, and 7) surface albedo. By knowing the above properties on an hourly basis, the surface temperature variation with time was estimated; hence from the surface temperature variation with time, assuming heat movement by conduction, the temperature variation at the lower soil depth was calculated.

## Literature Review

Very few reports, if any, have been previously published on research directly related to soil temperature profile determination using an energy budget approach. Most studies have used the energy budget equation to determine evaporation rates from a drying soil.

Penman (1956) utilized the energy budget equation for estimating evaporation rates. He utilized the aerodynamic equation for evaporation and sensible heat flux. He stated that evaporation is a physical process that must satisfy two basic requirements. There must be an energy supply and some transport mechanism to remove the water vapor.

Appleby (1958) made a study of the energy budget that is similar in nature to the current study. The purpose of the study was to investigate the validity of Halstead's model (1957) of the energy

budget at the earth/air interface programmed for an analog computer. The equations developed by Halstead were used as a basis to predict the distribution of wind, temperature, humidity, and the fluxes of heat, momentum, and water vapor. Halstead combined the available knowledge of the interactions among the processes of heat transfer by radiation, soil conduction, atmospheric convection, and evaporation and attempted to make micrometorological forecasts by quantitatively solving for the four fluxes in the surface energy budget equation.

Suomi and Tanner (1958) estimated the evapotranspiration from a crop from the disposition of solar and sensible energy available at the earth/air interface. Measurements of the heat budget including net radiation, heat transfer by soil conduction, air temperature gradient above the crop, and vapor pressure gradient above the crop were used in the Bowen equation to determine evapotranspiration rates which were then compared to lysimeter readings.

Lemon (1959) conducted studies and field experiments to evaluate the influence of the various boundary characteristics on the energy budget at the earth's surface. Net radiation, sensible heat flux, and soil heat flux were measured in order to determine evaporation from the equation $E = Rn - S - H$.

Fritschen and van Bavel (1962) determined the components of the surface energy balance equation over a wet bare soil surface. Evaporation rate was determined from the change in weight of two lysimeters. Net radiation was measured using miniature net radiometers and soil heat flow was measured with heat-flow transducers located in the center of the lysimeters. The sensible heat flux was then calculated

as a residual component of the energy balance equation. The study showed initially a high evaporation rate, and as drying continued evaporation declined and more energy was utilized to heat the soil and the air.

Tanner (1960), using the energy balance approach to determine evapotranspiration from crops, found that the heat exchange at the surface was 30 percent to 40 percent of the total radiation measured.

Tanner and Pelton (1960) estimated the potential evaporation rate using the approximate energy balance of Penman in which the net radiation Rn, had to be known.

Tanner and Lemon (1962) studied the amount of net radiation R, that is used for evapotranspiration from a cornfield. They found that for a 24-hour period with a moist soil up to 84 percent of R goes into evapotranspiration.

During the late spring of 1961, van Bavel, Fritschen, and Reginato (1963) carried out four experiments at the Water Conservation Laboratory in Phoenix, Arizona. In the first experiment the energy balance of an irrigated lysimeter surrounded by dry soil was studied. The second experiment involved laying a sheet of polyethylene on the surface of the lysimeter and ponding water. The third experiment involved irrigating the field surrounding the lysimeter and again ponding water on polyethylene. The fourth experiment involved the wet field and a removal of the polyethylene and irrigation of the lysimeter. In each case the appropriate energy balance equation was written and the variation of the components was measured as drying occurred. They

found the progressive drying of the soil surface affects the energy balance profoundly by increasing the albedo and surface temperature, and by decreasing the transport of soil moisture to the surface. In consequence, net radiation decreased, evaporation decreased, and heat flux from the surface into the air increased.

Sellers and Hodges (1962) developed a fluxometer for estimating latent heat from bare soil and short grass. The measured value of evaporation was then compared to the evaporation rate calculated using the energy balance approach.

Sellers (1964) calculated a potential evapotranspiration rate in arid regions using the energy balance equation. He solved the equation in terms of evaporation and two unknowns, surface temperature and surface vapor pressure, which were determined by trial and error.

Sellers (1965a) made an extensive study of the components of the surface energy balance equation at a cleared site near Tucson International Airport, Tucson, Arizona. The purpose of the study was two-fold: first, to obtain data on heat transfer from bare soil under stability conditions ranging from very stable to very unstable; and second, to check the accuracy of the fluxometer, previously mentioned, as an instrument for estimating the vapor flux from bare soil.

Dryden (1967) employed a modification of the fluxometer to determine the evaporation rate from a soil surface and then compared his estimates to the energy budget equation approach.

Fuchs and Tanner (1967) employed the energy budget equation to determine evaporation rates from a drying soil. Net radiation Rn, and

soil heat flux G, were measured. The sensible heat flux H, was determined utilizing the aerodynamic equation. The latent heat flux LE, then became the residual of the energy budget equation with all other variables being known. The soil surface temperature was determined using an infrared thermometer.

Van Bavel (1967) studied the surface energy balance of a drying soil and tested the Dalton equation for determination of evaporation and sensible heat flux. He found good agreement between actual and calculated evaporation rates, but failed to get acceptable calculated sensible heat flux rates.

Conaway and van Bavel (1967) utilized the aerodynamic equation to determine evaporation from a wet soil surface. The soil surface temperature was determined using an infrared thermometer. The soil surface vapor pressure was then determined from the surface temperature.

Welely, Thurtell, and Tanner (1970) determined the sensible heat flux using the eddy correlation technique. This was compared to energy budget estimates of the sensible heat flux.

## METHODS AND MATERIALS

The surface energy budget for a bare soil can be derived by considering a soil column extending from the surface to that depth where vertical heat exchange is negligible. The net rate G, at which the heat content of the soil column is changing is equal to the sum of the rates at which heat is added by the absorption of solar radiation $(Q + q)(1 - \alpha)$, by the absorption of longwave counter radiation from the atmosphere $I\downarrow$, by the downward transfer of sensible heat when the air is warmer than the surface -H, and by the horizontal transfer of heat into the column from the surroundings Fi, minus the rates at which heat is being lost by longwave radiation to the atmosphere $I\uparrow$, by the transfer of sensible heat to the air when the air is cooler than the surface H, by evaporation LE, where L is the latent heat of vaporization (590 cal $gm^{-1}$), and by the horizontal transfer of heat out of the column Fo. Written in equation form

$$G = (Q + q)(1 - \alpha) + I\downarrow - I\uparrow - H - LE + Fi - Fo$$

The terms $(Q + q)(1 - \alpha) + I\downarrow - I\uparrow$ form the radiation balance R, and subsurface heat flux into and out of the column is assumed to be zero, thus the energy balance equation becomes

$$G = R - H - LE$$

implying that the net available radiative energy is used to warm the air, evaporate water, and warm the soil. The above equation will be modified somewhat when a plant canopy is introduced over the bare soil.

The above equation can be written in terms of known variables and $\Delta T$, where $\Delta T$ is the air temperature T, minus the soil surface temperature Ts. Hourly measurements of air temperature, relative humidity, wind speed, incoming solar radiation, and cloud cover are needed to solve the previous equation. Soil temperature must also be recorded hourly for model validation purposes.

## Description of the Experimental Area

The experimental site was located in the Santa Rita Experimental Range approximately 35 miles south of Tucson, Arizona. The site was located in an area of predominantly blue grama [Bouteloua gracilis (HBK)] grass cover at an elevation of about 3000 feet above sea level. The layout of the experimental area is given in Figure 1, and consisted of two plots, 2.4 m by 2.4 m. Borders were laid on June 6, 1970 consisting of 12.5 cm by 24 cm boards buried approximately 7 cm into the ground. Backfill was placed both inside and outside the border to halt any leakage from plot irrigation. One plot was cleared of all vegetation Plot I, and the other was left in its natural state Plot II. The soil, classified as a sandy loam (Soil Conservation Service 1970), was initially very powdery, loose, and dry. Approximately 200 liters of water were applied to each on June 6, 1970 to facilitate the installation of thermocouples.

## Atmospheric Variables

The following variables were measured hourly for the duration of each experimental run period.

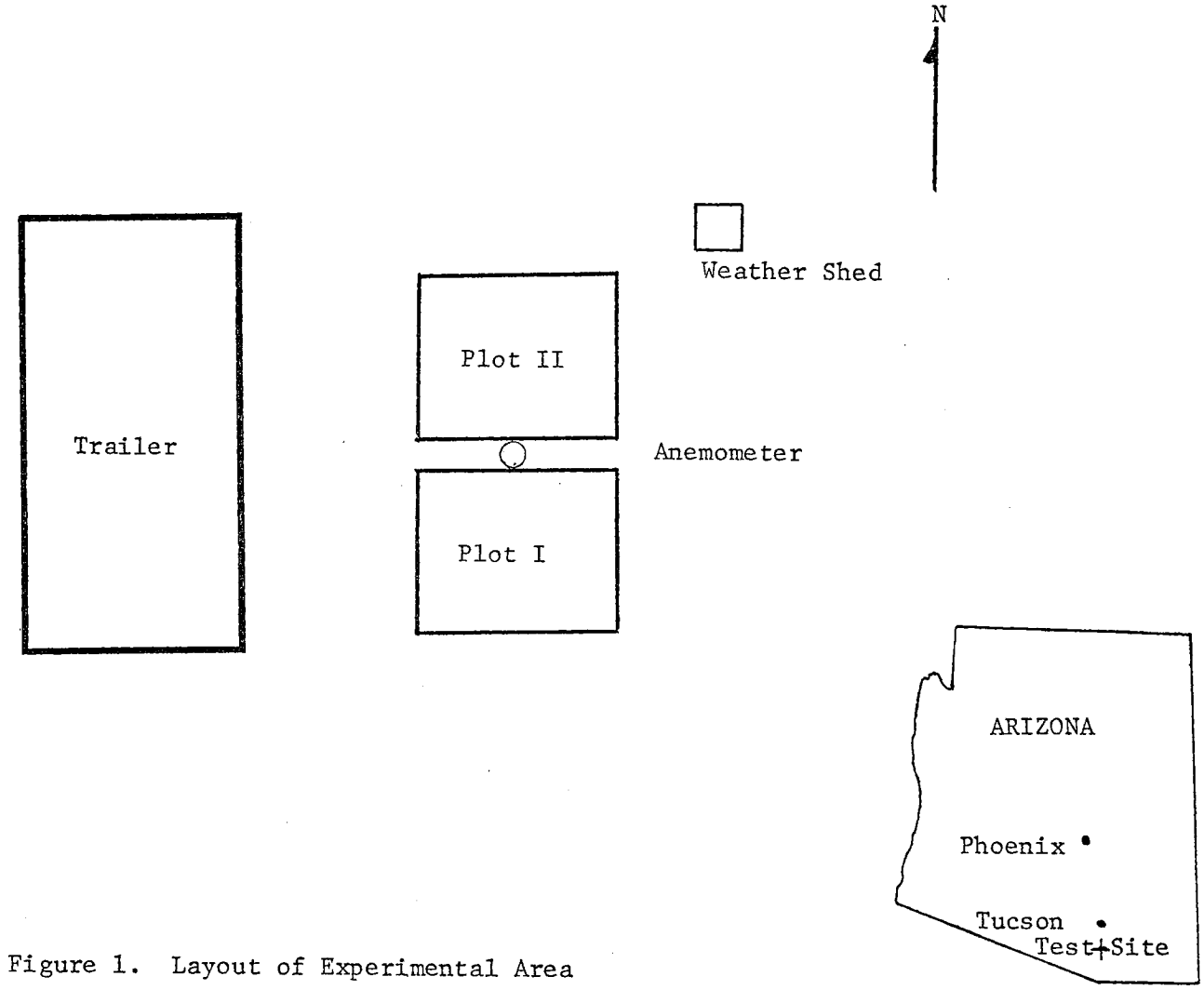


Figure 1. Layout of Experimental Area

Air Temperature

Air temperature measurements were taken at a height of 1.8 m using a Belfort Instrument Company chart recorder housed in a standard U.S. Weather Bureau shed adjacent to the plots.

Relative Humidity

Relative humidity measurements were made using the same Belfort recorder from which air temperature measurements were taken.

Wind Speed

Wind speed data were taken from a Meterological Research, Inc. anemometer which drove a strip recorder. Measurements were taken in miles wind run per hour and converted to centimeters per second. The anemometer was erected near the plots away from all obstructions at a height of 1.8 m.

Incoming Solar Radiation

An attempt to use incoming solar radiation data from The University of Arizona failed to give satisfactory results with the model. Afternoon scattered cloud cover caused discrepancies in incoming radiation between the research site and the University. To overcome the problem, a small, portable Belfort pyrheliometer was placed at the research site and calibrated with the Eppley pyranometer located at the University using data for three consecutive clear days. The pyrheliometer showed a definite time-lag response in the afternoon hours which was corrected by use of a correction factor. Table 1 shows the hour (MST) and the correction factor applied. The radiation value

Table 1. Pyrheliometer Correction Factor

| Time | Factor | Time | Factor |
|---|---|---|---|
| 0100 | 1.00 | 1300 | 1.05 |
| 0200 | 1.00 | 1400 | 1.11 |
| 0300 | 1.00 | 1500 | 1.16 |
| 0400 | 1.00 | 1600 | 1.18 |
| 0500 | 1.00 | 1700 | 1.59 |
| 0600 | 1.00 | 1800 | 1.10 |
| 0700 | 1.00 | 1900 | 1.60 |
| 0800 | 1.32 | 2000 | 1.00 |
| 0900 | 1.29 | 2100 | 1.00 |
| 1000 | 1.14 | 2200 | 1.00 |
| 1100 | 1.02 | 2300 | 1.00 |
| 1200 | 1.02 | 2400 | 1.00 |

obtained from the pyrheliometer was multiplied by the given factor for the corresponding hour.

### Cloud Cover

Cloud cover data were taken from the United States Weather Bureau located at Tucson International Airport. The airport is located approximately 20 miles north of the research site.

## Soil Properties

In order to determine the temperature response of a soil column, the thermal diffusivity must be known. The diffusivity determines the heating or cooling rate accompanying a given temperature profile.

### Thermal Diffusivity

A simple, approximate method to compute the thermal diffusivity K, of a soil from soil temperature variations is to assume the soil surface temperature T(0,t) at time t is given by

$$T(0,t) = \bar{T} + \Delta To \sin\omega t \tag{1}$$

The solution to the one-dimensional heat flow equation

$$\frac{\partial T}{\partial t} = K \frac{\partial^2 T}{\partial z^2} \tag{2}$$

given the above boundary condition is

$$T(z,t) = \bar{T} + \Delta T_o \, e^{-z(\omega/2\,k)^{1/2}} \sin\left[\omega t - (\omega/2\,k)^{1/2} z\right] \tag{3}$$

where T(z,t) is the temperature at depth z at time t.

The term $A = T_o e^{-z(\omega/2k)^{1/2}}$ represents the amplitude of the temperature wave at depth z. From the ratio of the amplitudes at two depths, the diffusivity K, can be calculated.

$$\frac{A1}{A2} = \exp[(z2 - z1)(\omega/2K)^{1/2}] \tag{4}$$

or

$$K = \frac{\omega}{2}\left[\frac{z2 - z1}{\ln A1/A2}\right]^2 \tag{5}$$

Jackson and Kirkham (1958), Wiernega, Nielsen, and Hagan (1969), and others have used the above approach to determine soil thermal diffusivity.

The thermal diffusivity can also be determined if the thermal conductivity $\lambda$, and the volumetric heat capacity C, are known by utilizing the formula $K = \lambda/C$. De Vries (1952) gave the following formula for the calculation of the thermal conductivity of moist soils.

$$\lambda = \frac{Xw\lambda w + Xs\lambda sks + Xa\lambda aka}{Xw + Xsks + Xaka} \tag{6}$$

where

X = the volume fraction with the subscripts s, w, and a referring to the solid material, water and air respectively

ks and ka = factors depending on the elliposidal shape of the soil particles

The thermal conductivity of the soil can also be measured <u>in situ</u> using a line heat source method (de Vries 1963a). A thin probe with a heating element and a thermocouple is inserted into the soil and a

known amount of current is supplied to the probe during a short time interval. The temperature of the probe increases and is measured with the thermocouple in the probe using a potentiometer. The temperature rise of the probe depends on the rate at which heat is conducted away from the probe and therefore on the thermal conductivity of the soil around the probe.

The thermal conductivity of a soil varies greatly with the moisture content as shown in Figure 2. De Vries (1963b) lists values for the thermal conductivity of various soil constituents as shown in Table 2. Generally the thermal conductivity varies from 4 mcal $cm^{-1}$ $sec^{-1}$ $°C^{-1}$ at 8 percent moisture content by volume to 5.5 mcal $cm^{-1}$ $sec^{-1}$ $°C^{-1}$ at 20 percent moisture content by volume.

The heat capacity is easier to determine and can be calculated from the general equation

$$C = XsCs + Xw \tag{7}$$

where

Xs = the volume fraction of solid material

Xw = the volume fraction of water

$$Cs = \frac{XmCm + XoCo}{Xs} \tag{8}$$

Xo = the volume fraction of organic material

Co = the heat capacity of minerals

Cm = the heat capacity of organic material

The heat capacity for a sandy soil generally ranges from 0.3 cal $cm^{-3}$ $°C^{-1}$ to 0.7 cal $cm^{-3}$ $°C^{-1}$ depending on soil moisture content.

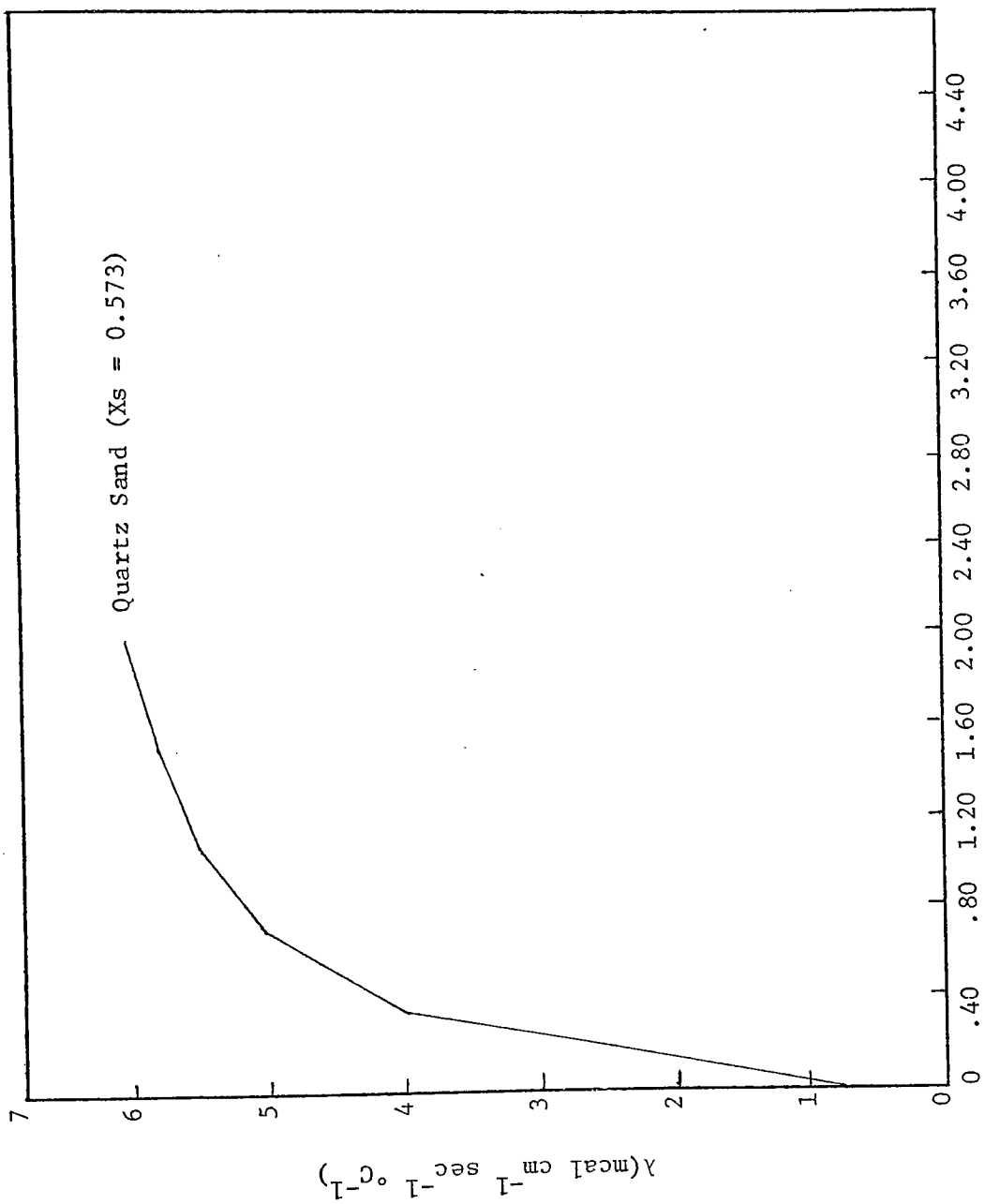


Figure 2. Thermal Conductivity Versus Soil Moisture Content

Table 2. Thermal Conductivity of Various Soil Constituents*

| Substance | T °C | (mcal $cm^{-1}$ $sec^{-1}$ $°C^{-1}$) |
|---|---|---|
| Quartz | 10 | 21 |
| Clay | 10 | 7 |
| Organic Matter | 10 | 0.6 |
| Water | 10 | 1.37 |
| Air | 10 | 0.06 |

* After Sellers 1965b.

The soil thermal diffusivity term must reflect the change of both the thermal conductivity and the volumetric heat capacity with soil moisture content. Figure 3 shows the relationship between water content and thermal diffusivity for a quartz sand, and according to Sellers (1965b) and Moench and Evans (1970) the thermal diffusivity of most soils lies between 0.001 and 0.012 $cm^2$ $sec^{-1}$. The thermal diffusivity for the plots studied was not directly measured, as this could possibly entail a complete study within itself. Rather, the main objective was to determine how well the model could simulate temperature profiles with as few field measurements as possible. The soil thermal diffusivity was calculated hourly using the empirical formula

$$K = [(C\lambda)^{1/2}/C]^2 \qquad (9)$$

where

$(C\lambda)^{1/2}$ = the thermal property of the soil

$C$ = the heat capacity of the soil

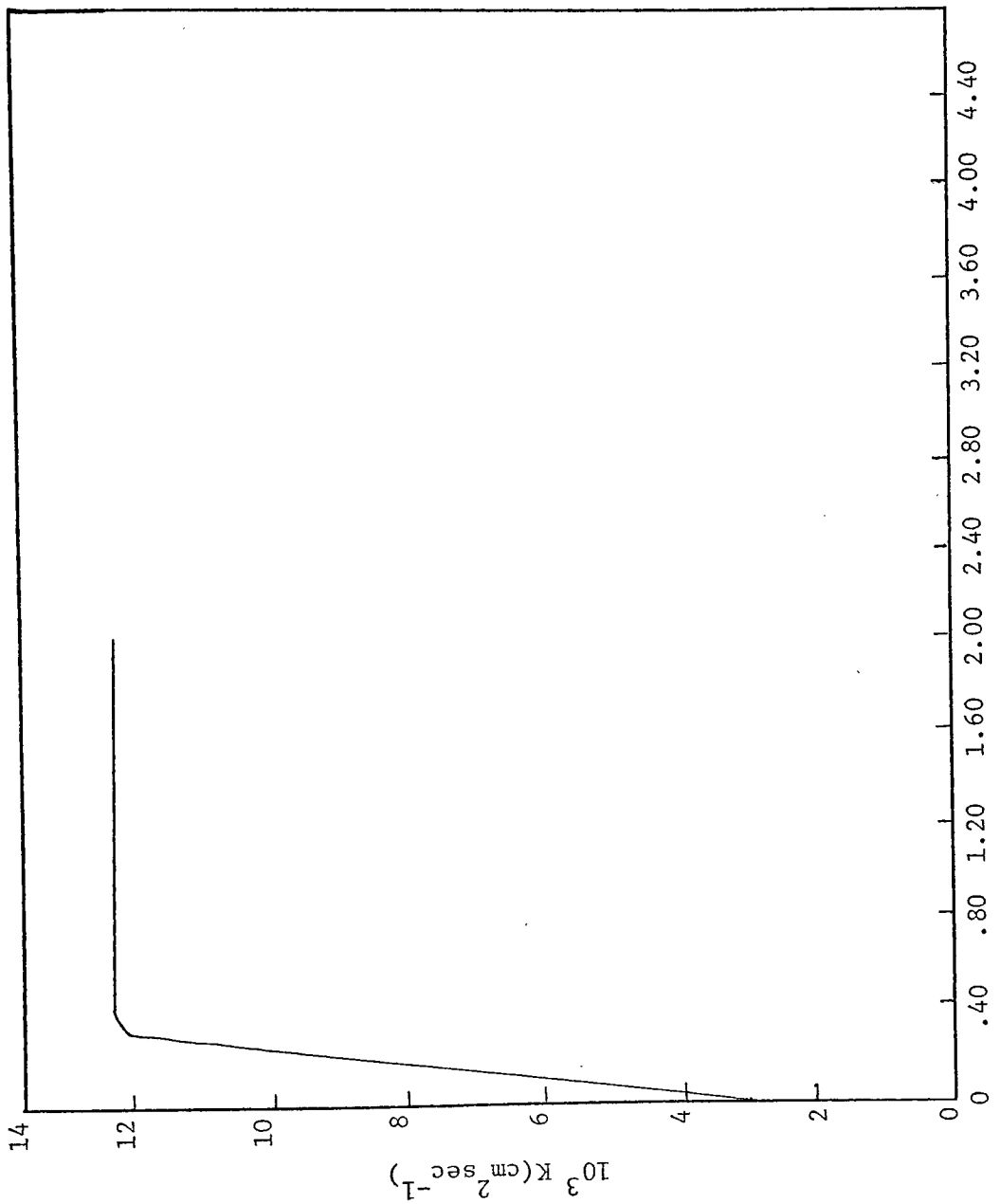


Figure 3. Thermal Diffusivity Versus Soil Moisture Content

The term $(C\lambda)^{1/2}$ is called the thermal property by Sellers (1965b) and will be used in establishing the magnitude of the flux into the soil accompanying the thermal regime. The range of values of the thermal property between wilting point and field capacity is fairly small, from 0.033 to 0.048 ly $°C^{-1}$ $sec^{-1/2}$ for sand. If the heat capacity ranges from 0.3 to 0.7 cal $cm^{-3}$ $°C^{-1}$, then a theoretical range of the thermal diffusivity can be calculated. The equation used to calculate the thermal property is given by

$$(C\lambda)^{1/2} = 0.0125 + 0.05\ [\tanh(1.5\ w_1/w_m)] \tag{10}$$

where

$w_1$ = the initial soil moisture content adjusted hourly

$w_m$ = the soil moisture content at field capacity (0.5 cm of water)

Likewise the equation used to calculate the heat capacity is given by

$$C = 0.20 + Xw \tag{11}$$

The above equations yield a thermal diffusivity value ranging from .004 to .006 $cm^2$ $sec^{-1}$ which is within the boundary of given literature values (Jackson and Kirkham 1958).

Soil Temperature Measurement

Soil temperatures were measured at two locations within each of the plots. Temperature measurements were taken at the surface and at 5 cm intervals down to 70 cm. Each measurement was replicated twice from the surface down to 35 cm. The temperature profile was measured using copper-constantan thermocouples. The thermocouples

were inserted horizontally from a 15 cm diameter hole dug with a power auger. A 0.625 cm by 5 cm wooden stake with small holes drilled at the proper 5 cm intervals was inserted into the excavation, and the thermocouples were then placed through the holes into the vertical soil wall. The stake provided for thermocouple stability and protection from being dislodged from the wall as backfill was placed into the hole.

The thermocouples were attached to two Honeywell Electronik 15 24-channel recorders. A timer on the recorders allowed a 24-channel printout once each hour. Six minutes were required for all 24-channels to be recorded, thus the recording started on the hour and concluded at 6 minutes past the hour.

Soil Water Content

The moisture content of the upper 5 cm of soil in the two study plots was determined gravimetrically. Soil moisture samples were taken daily on the first run to monitor the changing water content with time, and for Runs II and III soil moisture content was determined only for the starting day of each test. Four samples were taken each day from Plot I during Run I, and an average soil moisture content was determined on a dry weight basis. The dry weight was then converted to cm of water Iw, using the formula

$$Iw = \frac{Pw\ (BD)\ d}{100\ \rho w} \tag{12}$$

where

Pw = the soil moisture content on a dry weight basis

BD = the soil bulk density (assumed to be 1.6 gm $cm^{-3}$)

d = cm of soil depth

$\rho w$ = the density of water (1 gm $cm^{-3}$)

Soil moisture samples were taken from Plot II only at the beginning of each experimental run. Table 3 gives the soil moisture content for both plots for the three run periods. Plot II had consistently higher initial soil moisture values than Plot I. Plot irrigation in all cases occurred the previous day before the initial soil sampling occurred. Due to the coarse nature of the soil and a higher radiation load, the one day lag in sampling allowed Plot I to dry at a faster rate by evaporation than did Plot II.

The parameter d, in Equation (15) may also be referred to as the active zone, or that depth in the soil to which evaporation occurs. Previous work by Richards, Gardner, and Ogata (1956), Wiegand and Taylor (1962), Gardner and Hanks (1966), and Cary (1967) has shown the active zone for a fine sandy loam to vary from 1 to 5 cm; however, due to the coarse nature of the soil in the experimental plots, the active zone was assumed to be 5 cm. The active zone for the plant cover was taken to be 20 cm after excavation in the plot substantiated this to be a reasonable rooting depth.

Table 3. Soil Water Content

| Date | Soil Moisture Content (cm of water in Active Zone) | |
|---|---|---|
| | Plot I | Plot II |
| Run I | | |
| 6-10-70 | 0.51 | 0.60 |
| 6-11-70 | 0.32 | |
| 6-12-70 | 0.25 | |
| 6-13-70 | 0.20 | |
| Run II | | |
| 8-7-70 | 0.64 | 0.72 |
| Run III | | |
| 9-10-70 | 0.70 | 0.75 |

# MODEL DERIVATION

Two models for determining soil temperature profiles were derived. The first model is for a bare soil, and the second model is for a soil beneath a plant canopy. Each model can be separated into two components. The first component may be classified as atmospheric and the second component as soil related. The subsurface temperature profiles are determined using a soil surface temperature boundary condition which is derived from the energy balance equation. The model components, except for the mathematical determination of the subsurface temperature profiles, were derived by Dr. William D. Sellers, Professor in the Institute of Atmospheric Physics, The University of Arizona.

## Bare Soil Energy Budget

As previously stated, each term in the energy budget equation $R = H + LE + G$, must be solved in terms of known variables and $\Delta T$. Table 4 contains the list of variables used in the derivation of both models.

### Net Radiation R

The net radiation R can be defined as the incoming solar radiation $Q + q$, minus the effective outgoing radiation from the earth's surface I. Not all incoming radiation reaching the earth's surface is absorbed. A portion of it is reflected and scattered back to space. The soil surface albedo $\alpha$, is defined as that portion of

Table 4. Model Variables

| Variables | Symbol | Units |
|---|---|---|
| Net radiation | R | ly/hr |
| Sensible heat flux | H | ly/hr |
| Soil heat flux | G | ly/hr |
| Latent heat flux | LE | ly/hr |
| Albedo | $\alpha$ | percent |
| Emissivity | $\epsilon$ | percent |
| Effective outgoing radiation | I | ly/hr |
| Stefan-Boltzmann constant | $\sigma$ | ly/min $^{\circ}K^4$ |
| Von Karman constant | k | |
| Transfer coefficient | $D_w$ | cm/hr |
| Soil surface roughness length | $z_{os}$ | cm |
| Plant roughness length | $z_{op}$ | cm |
| Air temperature | T | $^{\circ}F$ |
| Soil surface temperature | $T_s$ | $^{\circ}F$ |
| Plant temperature | $T_p$ | $^{\circ}F$ |
| Previous hours average surface temperature | $T_{s1}$ | $^{\circ}F$ |
| Previous days average surface temperature | $\bar{T}_s$ | $^{\circ}F$ |
| Initial soil moisture content | $w_{s1}$ | cm of water |
| Critical soil moisture content | $w_{ks}$ | cm of water |
| Initial available plant moisture | $w_{p1}$ | cm |
| Critical plant moisture content | $w_{kp}$ | cm |

Table 4--Continued

| Variables | Symbol | Units |
|---|---|---|
| Initial depth distribution of soil temperature | TDEP | °F |
| Lower soil temperature boundary condition | $T_1$ | °F |
| Cloud cover | N | tenths |
| Wind speed | U | m/sec |
| Relative humidity | RH | percent |
| Precipitation | P | mm |

the incoming solar radiation reflected and varies from 5 to 45 percent. A moist soil has a low surface albedo because of its dark color. A dry soil, on the other hand, has a light color and hence a high reflectivity. The incoming solar radiation absorbed at the earth's surface becomes $(Q+q)(1-\alpha)$.

The surface of the earth, when heated by the absorption of solar radiation, becomes a source of longwave radiation which is a function of surface emissivity $\varepsilon$ and temperature $T_s$. A portion of the longwave radiation is reradiated back to earth in the form of counter radiation $I\downarrow$. Thus, the effective outgoing radiation $I_o$, is the difference between the outgoing and counter radiation. The equation for net radiation then becomes

$$R = (Q+q)(1-\alpha) - I_o \tag{13}$$

The components of the effective outgoing radiation can be determined by direct measurement or by empirical equations derived from data provided by the measurements. One such equation is the Relative Humidity Equation (Sellers 1965b) given by

$$I_o = \varepsilon(0.165 - 0.000769RH) \text{ ly min}^{-1} \tag{14}$$

where

$\varepsilon$ = the surface emissivity (0.90)

RH = the surface relative humidity in percent

The above equation must be modified if the sky is not clear. Clouds increase the counter radiation which decreases the effective outgoing radiation. The above equation must then be modified (Sellers 1965b) to give

$$I = I_o(1 - kn^m) \tag{15}$$

where

k,m = constants

n = the cloud cover in tenths

The quantity (1 - k) is a function of cloud height and type. Table 5 gives the quantity for various cloud types and heights.

Table 5. Ratio of Effective Outgoing Radiation with Overcast Skies (n = 1) to that with Clear Skies*

| Cloud Type | Height (m) | 1 - k |
|---|---|---|
| Cirrus | 12,200 | .84 |
| Cirrostratus | 8,390 | .68 |
| Altocumulus | 3,660 | .34 |
| Altostratus | 2,140 | .20 |
| Stratocumulus | 1,220 | .12 |
| Stratus | 460 | .04 |
| Nimbostratus | 92 | .01 |
| Fog | 0 | .00 |

* After Sellers 1965b.

The relative humidity used in Equation (14) is measured from a height of 1.8 m instead of the surface. If large temperature differences occur between the two heights, errors in calculating the effective outgoing radiation may occur. Hence, Sellers (1965b) showed the true effective outgoing radiation $I_s$, is approximated by

$$I_s = I + 4\varepsilon\sigma T^3(T_s - T) \tag{16}$$

where

$T$ = the air temperature measured at 1.8 m

$T_s$ = the surface temperature

$\sigma$ = the Stefan-Boltzmann constant ($8.14 \times 10^{-11}$ ly $min^{-1}$ $K^{-4}$)

Thus the final form of Equation (13) becomes

$$R = (Q+q)(1-\alpha) - I_o(1 - kn^m) - 4\varepsilon\sigma T^3 \Delta T \tag{17}$$

A compatible form of Equation (17) to be combined with the remaining energy budget components is given by

$$R = a_1 - a_2 - a_3\Delta T \tag{18}$$

where

$a_1 = (Q+q)(1-\alpha)$

$a_2 = I_o(1 - kn^m)$

$a_3 = 4\varepsilon\sigma T^3$

Sensible Heat Flux H

Assuming forced convection the sensible heat flux H, may be calculated by the aerodynamic equation

$$H = \frac{\rho C_p k^2 u \Delta T}{(\ln z/z_o)^2} \tag{19}$$

where

$\rho$ = the density of air

$C_p$ = the specific heat of air (.24 cal $gm^{-1}$ $°K^{-1}$)

$k$ = the Von Karman constant (.4)

$u$ = the wind speed measured at 180 cm

$z$ = the height at which wind speed is measured

$z_o$ = the roughness length (cm)

The term $k^2u(\ln z/z_o)^{-2}$ is commonly called the momentum transfer coefficient $D_m$. The density of air $\rho$, can be replaced by $p/RT$ where p is the atmospheric pressure in mb, R is the gas constant for dry air ($2.8704 \times 10^6$ erg-gm$^{-1}$°K$^{-1}$), and T is the air temperature. Thus Equation (19) becomes

$$H = \frac{p\, C_p\, D_m\, (T_s - T)}{RT} \tag{20}$$

or $a_4 \Delta T$.

Latent Heat Flux LE

The equation used to describe the transfer of latent heat is given by

$$LE = \frac{0.622\, \rho\, L\, D_w\, (e_s - e_z)\, a}{p} \tag{21}$$

where

$L$ = the latent heat of condensation

$D_w$ = the transfer coefficient

$e_s$ = the vapor pressure at the surface in mb

$e_z$ = the vapor pressure at elevation z in mb

$a$ = constant depending on the soil moisture content

Two stages of evaporation from soil are normally considered. In the first stage, when the soil moisture content w, is greater than some critical value $w_{ks}$, evaporation proceeds at about the potential rate $E_o$, and is dependent mainly on external meterological factors. In the

second stage, when the soil moisture content is less than the critical value $w_{ks}$, the evaporation rate depends on the moisture content of the soil.

The constant a, given above then becomes 1 for $w \geq w_{ks}$ and $w/w_{ks}$ for $w < w_{ks}$. Equation (21) must be solved for two cases corresponding to the two values that the constant a, may possess.

Case I a = 1:

An immediate concern in Equation (21) is the elimination of the surface vapor pressure. This may be eliminated using the finite difference form of the Clausius-Clapeyron equation

$$(e_s - e_{sa}) = \frac{0.622\ L\ e_{sa}}{RT^2}\ (T_s - T) \tag{22}$$

where

$e_{sa}$ = the saturation vapor pressure at air temperature

If the vapor pressure of the air at temperature T, is added and subtracted from Equation (22), the equation becomes

$$e_s - e_{sa} + e_z - e_z = \phi(T_s - T) \tag{23}$$

where

$e_z$ = the vapor pressure of the air at z cm at temperature T

$$\phi = \frac{0.622\ L\ e_{sa}}{RT^2}$$

or

$$(e_s - e_z) = \phi(T_s - T) + (e_{sa} - e_z) \tag{24}$$

Substituting Equation (24) into Equation (21) yields

$$LE = \frac{0.622\ L\ D_w}{RT} [\phi(T_s - T) + (e_{sa} - e_z)] \tag{25}$$

If $a_6 = \frac{0.311\ D}{RT} (e_{sa} - e_z)$ and $a_{12} = \frac{0.311\ D}{RT} \phi$ then Equation (25) becomes

$$LE = 2(a_{12}\ \Delta T + a_6)L \tag{26}$$

Case II $a = w/w_{ks}$:

Equation (21) must be solved again using $w/w_{ks}$ as the value of a. Before this can proceed, $a = w/w_{ks}$ must be altered somewhat. The soil moisture content w, may be defined as the average moisture content over a period. If $w_{s1}$ is the moisture content at the beginning of a period and $w_{s2}$ is the moisture content at the end of the period, then w is equal to $0.5\ (w_{s1} + w_{s2})$. The moisture budget equation

$$S = p - E + w_{s1} - w_{s2} \tag{27}$$

where

S = the moisture surplus or runoff

p = the rainfall

E = the evaporation

is also employed. If the assumption is made that no runoff or rainfall will occur during the test period, then Equation (27) becomes

$$w_{s1} = w_{s2} + E \tag{28}$$

If $w_{s2} = w_{s1} - E$ is substituted into $w = 0.5\ (w_{s1} + w_{s2})$, the constant a becomes

$$a = 0.5\ (w_{s1} + w_{s2})/w_{ks} \text{ or } 0.5\ (2w_{s1} - E)/w_{ks} \tag{29}$$

The value of a shown in Equation (29) is then substituted back into Equation (21) yielding

$$LE = \frac{0.311\ \rho\ L\ D}{p}\ (2w_{s1} - E)\ \ [(T_s - T) + e_{sa} - e]/w_{ks} \tag{30}$$

Equation (30) is manipulated to give a result similar to Equation (26). Equation (30) becomes

$$LE\ [w_k + \frac{.311\ D\ (T_s - T)}{RT}\ \phi + \frac{.311\ D\ (e_{sa} - e_z)}{RT}] = \frac{.622\ L\ D_w\ (T_s - T)}{RT}\ w_{s1} + \frac{.622\ L\ D\ w_{s1}(e_{sa} - e_z)}{RT} \tag{31}$$

Letting $a_6$ and $a_{12}$ equal the previously given values, Equation (31) becomes

$$LE = \frac{2\ L\ w_{s1}\ (a_6 + a_{12}\ \Delta T)}{(w_k + a_{12}\ \Delta T + a_6)} \tag{32}$$

Equations (26) and (32) become the final forms of the latent heat flux equation.

Denmead and Shaw (1962) reported that plants begin transpiring below the potential rate when 75 percent of the initial moisture content is reached, therefore $w_{ks}$ is assumed equal to $.75\,w_{s1}$ for both models.

Soil Heat Flux G

The rate at which heat flows through a soil is directly proportional to the temperature gradient at that depth. At depth z

$$G = -\ \lambda\ \frac{\Delta T}{\Delta Z} \tag{33}$$

where flow is positive downward when the temperature decreases with depth. The constant $\lambda$, represents the rate at which energy passes through unit area of a substance when a temperature gradient of 1°C $cm^{-1}$ exists.

Use once again must be made of the one-dimensional heat conduction equation given as Equation (2)

$$\frac{\partial T}{\partial t} = \frac{K\partial^2 T}{\partial Z^2}$$

where $K = \lambda/c$ is the thermal diffusivity. The above equation can be solved for the case of a homogeneous semi-infinite soil whose surface is heated in a periodic manner. Assume that $T_s$ at time t is given by

$$T_s(t) = \bar{T}_s + \Delta T_o \sin\omega t \tag{34}$$

where

$T_s(t)$ = the surface temperature at time t

$\bar{T}_s$ = the mean daily soil temperature

$\Delta T_o$ = the amplitude of the surface temperature wave

$\omega$ = the angular frequency of oscillation ($2\pi/24$ for a 24 hour period)

Using the above boundary condition, Carslaw and Jaeger (1959) show the solution to Equation (2) to be

$$T(z,t) = \bar{T} + \Delta T_o \, e^{-z(\omega/2K)^{1/2}} \sin\left(\omega t - (\omega/2K)^{1/2} z\right)$$

where

$T(z,t)$ = the soil temperature at depth Z at time t

Sellers (1965b) shows that Equations (33) and (2) can be combined to give

$$G(z,t) = \Delta T_o (\omega C\lambda)^{1/2} \, e^{-z(\omega/2K)^{1/2}} \sin [\omega t - (\omega/2K)^{1/2} z + \pi/4] \quad (35)$$

which is the basic equation used to determine $\Delta T$.

At the surface, $z = 0$ and Equation (35) reduces to

$$G(0,t) = \Delta T_o (\omega C\lambda)^{1/2} \sin (\omega t + \pi/4) \quad (36)$$

Making use of the trigonometric identity $\sin (s_1 + s_2) = \sin s_1 \cos s_2 + \cos s_1 \sin s_2$, Equation (36) can be expressed as

$$G = \Delta T_o \frac{\sqrt{2}}{2} (\sin \omega t + \cos \omega t) (\omega C\lambda)^{1/2} \quad (37)$$

If Equation (34) is solved for $\sin \omega t$, the equation becomes $\sin \omega t = (T_s - \bar{T}_s)/\Delta T_o$. The equation also yields a value for $\cos \omega t$ when differentiated with respect to t, $\cos \omega t = \partial T_s / \partial t \, \omega \Delta T_o$. Substituting these values back into Equation (37) gives

$$G = \frac{\sqrt{2}}{2} \Delta T_o \left[ \frac{T_s - \bar{T}_s}{\Delta T_o} + \frac{\partial T_s}{\partial t \omega \Delta T_o} \right] (\omega C\lambda)^{1/2} \quad (38)$$

or

$$G = \frac{\sqrt{2}}{2} \left[ T_s - \bar{T}_s + \frac{\Delta T_s}{\Delta t \omega} \right] (\omega C\lambda)^{1/2} \quad (39)$$

Adding and subtracting the air temperature T, inside the brackets and letting $\Delta T_s / \Delta t = T_s - T_{s1}$, Equation (39) becomes

$$G = \frac{\sqrt{2}}{2} (\omega C\lambda)^{1/2} (1 + 2/\omega) \Delta T + \frac{\sqrt{2}}{2} (\omega C\lambda)^{1/2} [T - \bar{T}_s + 2/\omega (T - T_{s1})] \quad (40)$$

where

$T_{s1}$ = the previous hours average surface temperature

The final form of Equation (40) used in the derivation is

$$G = [187.45(C\lambda)^{1/2}]\ \Delta T + 21.71(C\lambda)^{1/2}[T - \bar{T}_s + 7.64(T - T_{s1})] \qquad (41)$$

or $a_7\ \Delta T + a_8$.

The equations may now be combined to give $\Delta T$. Taking the computed equation for each component of the energy budget equation $R = H + G + LE$, and combining them for Case I yields

$$a1 - a2 - a3\ \Delta T = a4\ \Delta T + a7\ \Delta T + a8 + 2\ (a12\ \Delta T + a6)L \qquad (42)$$

Collecting terms and solving for $\Delta T$ yields

$$\Delta T = \frac{a1 - a2 - a8 - 2a6L}{a3 + a4 + 2a12L} \qquad (43)$$

The above equation gives $\Delta T$ for the case of the soil moisture content being above some critical value $w_{ks}$. Case II yields a somewhat more complex solution. The equation for Case II is

$$a1 - a2 - a3\ \Delta T = a4\ \Delta T + a7\ \Delta T + a8 + \frac{2(a12\ \Delta T + a6)Lws1}{w_{ks} + a12\ \Delta T + a6} \qquad (44)$$

Solving for $\Delta T$ yields a quadratic equation in the form

$$a12(a3 + a4 + a7)\Delta T^2 + 2Lw_{s1}a12\ \Delta T + (w_{ks} + a6)(a3 + a4 + a7)\Delta T - a12(a1 - a2 - a8)\Delta T - (w_{ks} + a6)(a1 - a2 - a8) + 2Lw_{s1}a6 = 0 \qquad (45)$$

If new variables b3, b4, and b5 are defined, Equation (45) can be reduced to

$$\Delta T = \frac{-b4 \pm \sqrt{b4^2 - 4\ b3b5}}{2b3} \tag{46}$$

where

$$b3 = a12(a3 + a4 + a7)$$

$$b4 = a12(a1 - a2 - a8) - (w_k + a6)(a3 + a4 + a7) - 2Lw_{s1}a12$$

$$b5 = (w_{ks} + a6)(a1 - a2 - a8) - 2lw_{s1}a6$$

As previously stated, $\Delta T$ is the difference between the surface temperature $T_s$, and the air temperature T. Thus, if $\Delta T$ is calculated hourly, and the corresponding T is known, then the resulting surface temperature can be calculated.

Effects of Plant Canopy on Soil Surface Energy Budget

If a plant canopy is introduced over the soil surface, the bare soil energy budget is altered significantly. In order to obtain a new solution to the energy budget equation, a basic simplifying assumption must be made concerning the canopy itself. The canopy is assumed to be a sheet suspended over the surface with openings in it corresponding to the amount of ground that can be seen looking directly down over the plant cover at the ground $\tau I$. This simplifies calculation of the transfer coefficient for sensible and latent heat flux. Although work has been done (Cionco 1963, Lemon 1967) to determine the transfer coefficient within a plant canopy, the solution is mathematically involved. The log law for the wind profile with a varying roughness length will be assumed to be adequate for transfer coefficient calculation.

An energy balance equation for both the plant surface and the soil surface must be written. Each equation will yield $\Delta T_p$ and $\Delta T_s$ where $\Delta T_p = T_p - T_a$ and $\Delta T_s = T_s - T_a$. $T_p$ is the plant surface temperature, $T_s$ is the soil surface temperature, and $T_a$ is the ambient air temperature. Each equation will be considered for two cases. The soil surface energy budget will consider two stages of evaporation: 1) $w_s > w_{ks}$, and 2) $w_s \leq w_{ks}$. The plant surface energy budget will also consider two stages of evapotranspiration: 1) $w_p > w_{kp}$, and 2) $w_p \leq w_{kp}$. Plant evapotranspiration rate is assumed to be regulated solely by soil moisture conditions and not stomata opening or closure. Solving each equation for the two stages gives rise to three sets of possible solutions: 1) $w_s \geq w_{ks}$, $w_p > w_{kp}$; 2) $w_s < w_{ks}$, $w_p > w_{kp}$; and 3) $w_s < w_{ks}$, $w_p < w_{kp}$. The case of $w_p \leq w_{kp}$ and $w_s > w_{ks}$ is not treated.

The energy balance equation beneath a plant canopy is considerably more complex to solve, thus its derivation will be presented in Appendix A and only the final equations for the three sets of possible solutions will be given here.

Solution I: $w_s \geq w_{ks}$, $w_p \geq w_{kp}$

$$\Delta T_p = \frac{b2b3' + b1'b3}{b1b1' = b2b2'} \tag{47}$$

$$\Delta T_s = \frac{b2' \ \Delta T_p + b3'}{b1'} \tag{48}$$

Solution II: $w_s < w_{ks}$, $w_p \geq w_{kp}$

$$\Delta T_p = \frac{b2 \ \Delta T_s + b3}{b1} \tag{49}$$

$$\Delta T_s = \frac{-b16 \pm (b16^2 - 4b15b17)^{1/2}}{2b15} \tag{50}$$

Solution III: $w_s < w_{ks}$, $w_p < w_{kp}$

$$b4\ \Delta T_p^2 + (b5 + b6\ \Delta T_s)\ T_p + b7\ \Delta T_s + b8 = 0 \quad (51)$$

$$b11\ \Delta T_p^2 + (b12 + b13\ \Delta T_s)\ T_p + b9\ \Delta T_s^2 + b10\ T_s + b14 = 0 \quad (52)$$

The two unknowns, $\Delta T_p$ and $\Delta T_s$, are given in terms of ai, bi, ai', and bi' which represent known variables.

## Soil Temperature Calculation

The model derivation for the soil surface temperature may now be used to calculate the sub-surface temperature variation with time assuming heat movement by conduction. The equation describing heat transfer in a one-dimensional isotropic medium was given in Equation (2) as

$$\frac{\partial T}{\partial t} = K \frac{\partial^2 T}{\partial z^2}$$

where

T = the soil temperature at depth z

t = the time increment

z = the depth increment

K = the thermal diffusivity

Several problems are involved with use of the above equation. The volumetric heat capacity C, and the thermal conductivity $\lambda$, are not constant with soil-water content thus giving a K value that is not constant. Also, in the presence of temperature gradients, heat transfer takes place not only by conduction but by convection. Nonetheless, if the soil-water content distribution is uniform and essentially invariant

with time, Equation (2) may adequately describe soil temperature behavior.

Numerical Analysis

A simple difference equation approximating Equation (2)

$$\frac{T_j^{n+1} - T_j^n}{\Delta t} = \frac{K(T_{j+1}^n - 2T_j^n + T_{j-1}^n)}{(\Delta z)^2} \qquad (53)$$

where j is the depth interval and n is the time interval (Richmeyer and Morton 1967). The above equation was used to compute the soil temperature variation to 70 cm below the soil surface from known soil diffusivity, boundary, and initial conditions.

The temperature variation at the soil surface served as the upper boundary condition. The soil temperature at 70 cm was used as the lower boundary condition, and was found to be constant over the period of each experimental run. The initial distribution of temperature with depth must also be known. The limitation on the use of this equation in order to insure stability in the numerical solution is, according to Richmeyer and Morton (1967), that

$$\frac{2K\Delta t}{(\Delta z)^2} < 1$$

Since the soil temperature was measured every hour and the diffusivity has a value of approximately 0.005 $cm^2$ $sec^{-1}$, the stability criterion could not be met by taking $\Delta z$ = 5 cm. Thus a 30 minute soil surface temperature was used by taking the average of the hourly surface temperature. The $\Delta t$ term then became 1800 sec and $(\Delta z)^2 > 2(.005)$ or $\Delta z > \sqrt{18}$. In the computation z was always 5 cm.

## APPLICATION OF MODEL TO FIELD SITUATION

Three experimental runs were made during the summer of 1970. Each run was from 4 to 7 days in length, and in each case the plots were initially watered and soil temperature variation was measured over the drying period to compare with model predictions. The dates of the three runs were: June 10-13, August 8-14, and September 10-15.

### Run I--June 10-13, 1970

The bare soil and the grass covered plots were watered on the afternoon of June 8, 1970, and soil temperature monitoring began June 9 in Plot I and continued through June 14. Due to a malfunction in one recorder, only soil temperature variation for the bare soil was obtained during the test period. The model was applied for the period June 10-14 beginning at 1400 June 10. Several initial conditions were necessary and are given in Table 6 for the test period.

Table 6. Initial Conditions for Plot I (June 10-14, 1970)

| Symbol | Magnitude | Units |
|---|---|---|
| $W_{s1}$ | 0.51 | cm |
| $W_{sk}$ | 0.50 | cm |
| $T_{s1}$ | 102.00 | °F |
| $\bar{T}_s$ | 79.00 | °F |
| $Z_{os}$ | 0.75 | cm |

Figure 4 shows actual versus calculated soil temperature variation at 5 cm intervals from 5 cm to 30 cm for the period 1400, June 10 to 1300, June 14. The 5 cm peak temperature for June 10 occurred at 1500 while at 15 cm the peak occurred at 1800. The zone of high temperature originating at the surface propagated downward with decreasing intensity to the deeper soil layers. As it moved, it lost heat by conduction to the cooler soil above and below. The daily maximum temperature for the 5 cm depth increased from June 10 to June 11 then remained essentially constant. As the top soil dried out, its heating rate was impeded by the poor conductivity of the soil and the daily maximum tended to stabilize. The lower soil depths from 10 cm to 40 cm remained moist throughout the observation period and responded to the daily influx of heat by slowly becoming warmer for all time periods.

Table 7 gives the total daily values of net radiation R, sensible heat flux H, soil heat flux G, and latent heat flux LE, as calculated by the model from Equations (18), (29), (41), and (26), respectively. The equations give hourly values which are then summed over the 24 hour period. Also given in Table 7 is the measured average hourly values of cloud cover C, temperature T, wind speed U, relative humidity RH, and precipitation P. As seen from the table, the net radiation showed a steady decline from a peak of 535 ly $day^{-1}$ on June 10 to 204 ly $day^{-1}$ on June 14. This was due to 1) an increase in soil surface albedo which caused a greater reflection of the incoming solar radiation and 2) an increase in the outgoing longwave radiation. Approximately 82 percent of the net radiation on June 10 went into evaporation

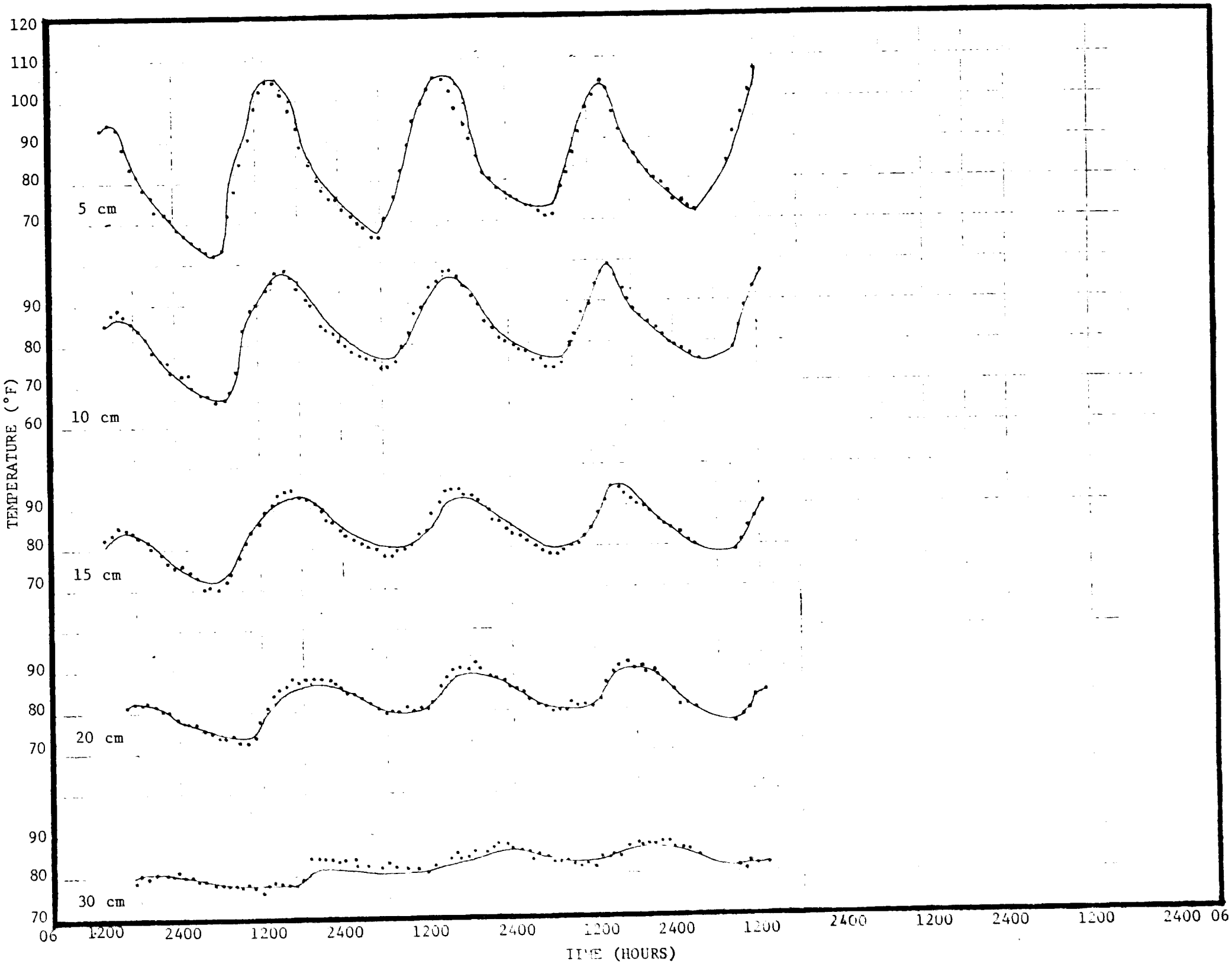


Figure 4. Actual (···) and Calculated (——) Soil Temperature Profiles for 1400 June 10 to 1300 June 14, 1970. Run I, Plot I.

Table 7. Total Daily Values in Langleys of Net Radiation R, Sensible Heat Flux H, Latent Heat Flux LE, Soil Heat Flux G, and Average Hourly Cloud Cover N (Tenths), Air Temperature T (°F), Wind Speed U (m $sec^{-1}$), Relative Humidity RH (Percent), and Precipitation P (mm), for Run I, Plot I

| Date | Plot | R | H | LE | G | N | T | U | RH | P |
|---|---|---|---|---|---|---|---|---|---|---|
| | I | | | | | | | | | |
| 6/10/70 | | 352.8 | 69.6 | 588.0 | -2.4 | 0.0 | 75.5 | 2.9 | 41.6 | 0.0 |
| 6/11/70 | | 297.6 | 290.4 | 2.4 | 4.8 | 0.0 | 77.5 | 4.3 | 42.8 | 0.0 |
| 6/12/70 | | 247.2 | 247.2 | 0.0 | 0.0 | 3.5 | 81.1 | 3.7 | 27.1 | 0.0 |
| 6/13/70 | | 211.2 | 208.8 | 0.0 | 2.4 | 4.3 | 77.8 | 2.4 | 31.7 | 0.0 |
| 6/14/70 | | 204.0 | 216.0 | 0.0 | -12.0 | 0.0 | 70.0 | 1.7 | 27.5 | 0.0 |

of water and 19 percent was used to heat the air above the plot. The additional 1 percent of energy was drawn from the soil mass itself to aid in evaporation and sensible heat flux. Almost 98 percent of the net radiation the second day went into sensible heat flux, the remainder being used to evaporate water from a rapidly drying soil and to heat the soil column. Average wind speed also increased on the second day which tended to increase the sensible heat flux due to additional turbulence. The remaining three days showed the net radiation inducing a large daily sensible flux with the remainder of the energy going to warm the soil. Evaporation had ceased after just two days of radiation input. The evaporation rate seemed to halt in a short period of time, but the initial soil moisture content at the beginning of the observation period was only approximately 0.5 cm of water. The soil also had a moderately coarse texture which does not lend itself to a large moisture holding capacity.

## Run II--August 8-14, 1970

The bare soil and grass covered plots were irrigated on the afternoon of August 7, 1970, and soil temperature monitoring began at 0800 the morning of August 7. The model was applied for the period August 8-14 beginning at 0800 August 8. Several initial conditions had to be known in order to apply the model for the given period. These are given in Table 8.

### Plot I

Figure 5 shows the actual versus calculated soil temperature variation for Plot I. Table 9 gives the total daily values of net

Table 8. Initial Conditions for Plot I and Plot II (August 8-14, 1970)

| Symbol | Magnitude | | Units |
|---|---|---|---|
| | Plot I | Plot II | |
| $W_{sl}$ | 0.64 | 0.72 | cm |
| $W_{sk}$ | 0.50 | 0.50 | cm |
| $W_{pl}$ | | 3.00 | cm |
| $W_{pk}$ | | 1.00 | cm |
| $T_{sl}$ | 80.0 | | °F |
| $\bar{T}_s$ | 82.0 | | °F |
| $T_{pl}$ | | 80.0 | °F |
| $\bar{T}_p$ | | 82.0 | °F |
| $Z_{op}$ | | 6.0 | cm |
| $Z_{os}$ | 1.0 | | cm |

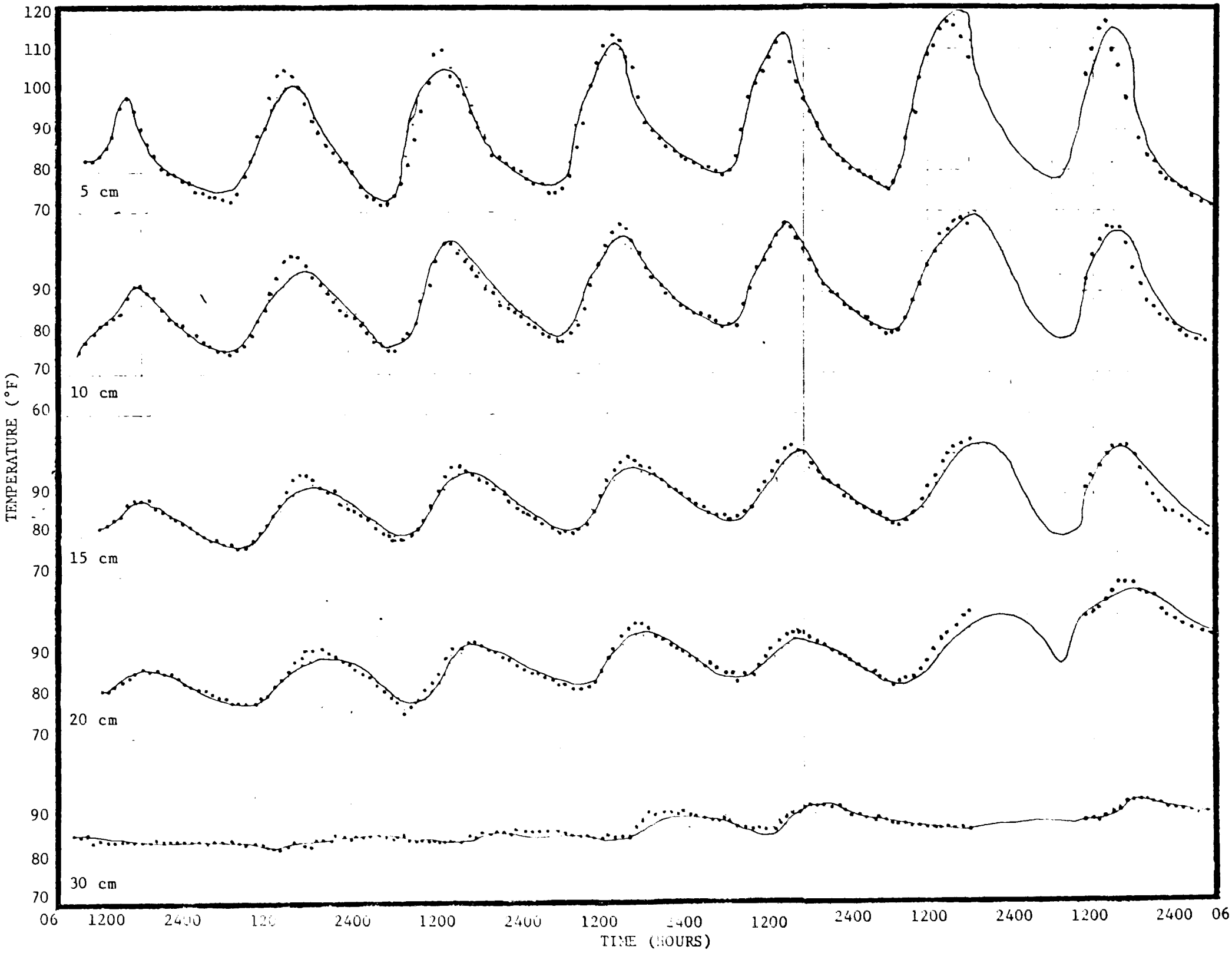


Figure 5. Actual (···) and Calculated (___) Soil Temperature Profiles for 0800 August 8 to 0700 August 15, 1970. Run II, Plot I.

Table 9. Total Daily Values in Langleys of Net Radiation R, Sensible Heat Flux H, Latent Heat Flux LE, Soil Heat Flux G, and Average Hourly Cloud Cover N (Tenths), Air Temperature T (°F), Wind Speed U (m $sec^{-1}$), Relative Humidity RH (Percent), and Precipitation P (mm), for Run II, Plot I

| Date | Plot | R | H | LE | G | N | T | U | RH | P |
|---|---|---|---|---|---|---|---|---|---|---|
| | I | | | | | | | | | |
| 8/8/70 | | 250.1 | -4.2 | 235.6 | 18.7 | 6.3 | 82.9 | 1.1 | 67.1 | 0.0 |
| 8/9/70 | | 215.9 | 48.0 | 115.0 | 52.9 | 7.7 | 82.4 | 1.4 | 68.0 | 0.0 |
| 8/10/70 | | 137.3 | 81.5 | 18.9 | 36.9 | 4.1 | 82.1 | 1.0 | 67.2 | 0.0 |
| 8/11/70 | | 131.8 | 122.5 | 1.8 | 7.5 | 7.5 | 82.9 | 1.4 | 64.7 | 0.0 |
| 8/12/70 | | 120.6 | 105.7 | 0.0 | 2.1 | 2.1 | 82.1 | 1.3 | 66.7 | 0.0 |
| 8/13/70 | | 142.5 | 126.5 | 0.0 | 1.5 | 1.5 | 86.1 | 1.2 | 55.0 | 0.0 |
| 8/14/70 | | 141.5 | 133.2 | 0.0 | 6.2 | 6.2 | 78.6 | 1.5 | 76.8 | 0.0 |

radiation R, sensible heat flux H, soil heat flux G, and latent heat flux LE, as calculated by the model. Also given in Table 9 is the measured average hourly values of cloud cover C, temperature T, wind speed U, relative humidity RH, and precipitation P. The values given in Table 9 help explain the soil temperature variation for August 8-14.

As seen in Figure 5, the observed and calculated temperature for August 8 agree very well. The temperature variation with depth shows about an hour lag in peak temperature occurrence for each 5 cm in depth. The latent heat flux LE, accounted for 94 percent of the net solar radiation R for the day. Additional energy was drawn from the air, 4.2 langleys, to aid the evaporation and soil heat flux process.

The temperature variation for August 9 shows a calculated lag and a lower peak temperature for the day than actually occurred. This may be explained by observing the average hourly cloud cover N, for the day. Table 9 shows an approximate value of 8 tenths or 80 percent average hourly cloud cover, however the data were from Tucson International Airport and variation between the site and the airport may have occurred. The time of significant difference between the actual and calculated soil temperature profiles occurred from 1300 to 1600. Cloud cover for these hours were 9, 6, 2, and 1 tenth, respectively. The actual soil temperature profiles seemed to respond to a cloud cover less than the 9 tenths and 6 tenths given for 1300 and 1400, thus the actual temperature is higher than the calculated temperature from 1300 to 1600. Table 9 shows 54 percent of the net radiation for the day was used for evaporating water. The amount of energy going into

heating the air above the soil surface and warming the soil column are essentially the same.

Figure 5 shows an improved agreement between the calculated and actual temperature profiles for August 10. The 15 cm depth shows a maximum difference between calculated and actual of only 2 degrees. Table 9 shows that the net radiation had declined from a maximum of 250 ly the first day to 137 ly on August 10. This is due to an increase in soil albedo from approximately 9 percent to 24 percent plus an increase in the outgoing longwave radiation. The energy used for evaporation is now only 14 percent of the total net radiation, as 62 percent of the energy is being used to warm the air above the soil surface and 24 percent being used to warm the soil surface.

Figure 5 again shows a deviation between actual and calculated temperatures from 1300 to 1700 for August 11. The average cloud cover for this period was 7.5 tenths or 75 percent thus raising the possibility of cloud cover variation between the site and Tucson International Airport. Table 9 shows an increasing amount of energy being used to warm the air above the soil. Soil heat flux was rather low, 7.5 ly; however a 3.2 cm $sec^{-1}$ average wind speed could account for the turbulence necessary to transfer sensible heat flux in greater amounts than soil heat flux.

Model prediction of soil temperature profiles for the remaining two days was generally good. Data was lost from 1900 August 13 to 1000 August 14 due to generator failure, however the calculated values are given for the period.

Hourly values of simulated energy balance components for August 8, 1970 are shown in Figure 6. The net radiation R, showed a steady increase from 0800 to 1000. The data at this time indicated cloud cover decreased the net radiation until 1300 at which time it increased until 1500. The net radiation at night showed a gradual decline in outgoing radiation as the soil surface slowly cools.

The latent heat flux accounted for a large portion of the net radiation during the daytime and also remained positive for the night hours, the energy for evaporation being drawn from the warm atmosphere and lower soil column. Positive evaporation from moist soil at night is not uncommon in dry arid regions (Sellers 1965b).

Sensible heat flux was positive until 1800 indicating the soil surface was warmer than the overlying air layer. Soil heat flux was also positive for the day until 1800, and the magnitude of the flux was greater than that for the sensible heat flux from 0800 to 1800. During this period the moist soil had a high thermal conductivity and responded rapidly to the radiation input.

Plot II

Figure 7 shows the actual versus calculated soil temperature variation beneath a 30 percent plant cover. The most apparent result, when comparing the temperature variation of Plot I and Plot II, was a temperature damping effect beneath the plant canopy. During the late morning and early afternoon hours the vegetation intercepted at least 30 percent of the incoming solar radiation, thus the peak surface temperature was reduced due to a lower radiation load. At night the

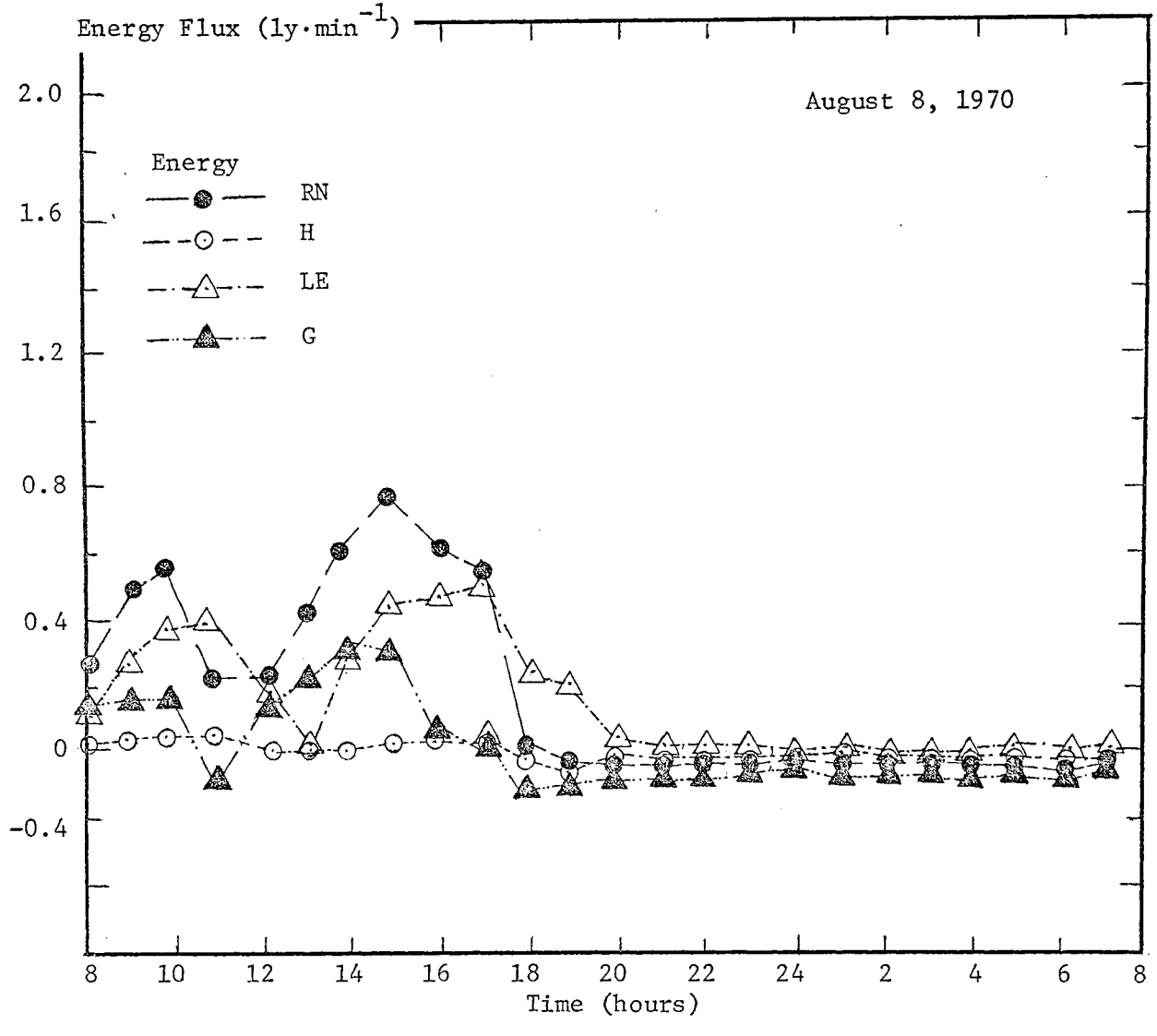


Figure 6. Hourly Values of Simulated Energy Balance for August 8, 1970

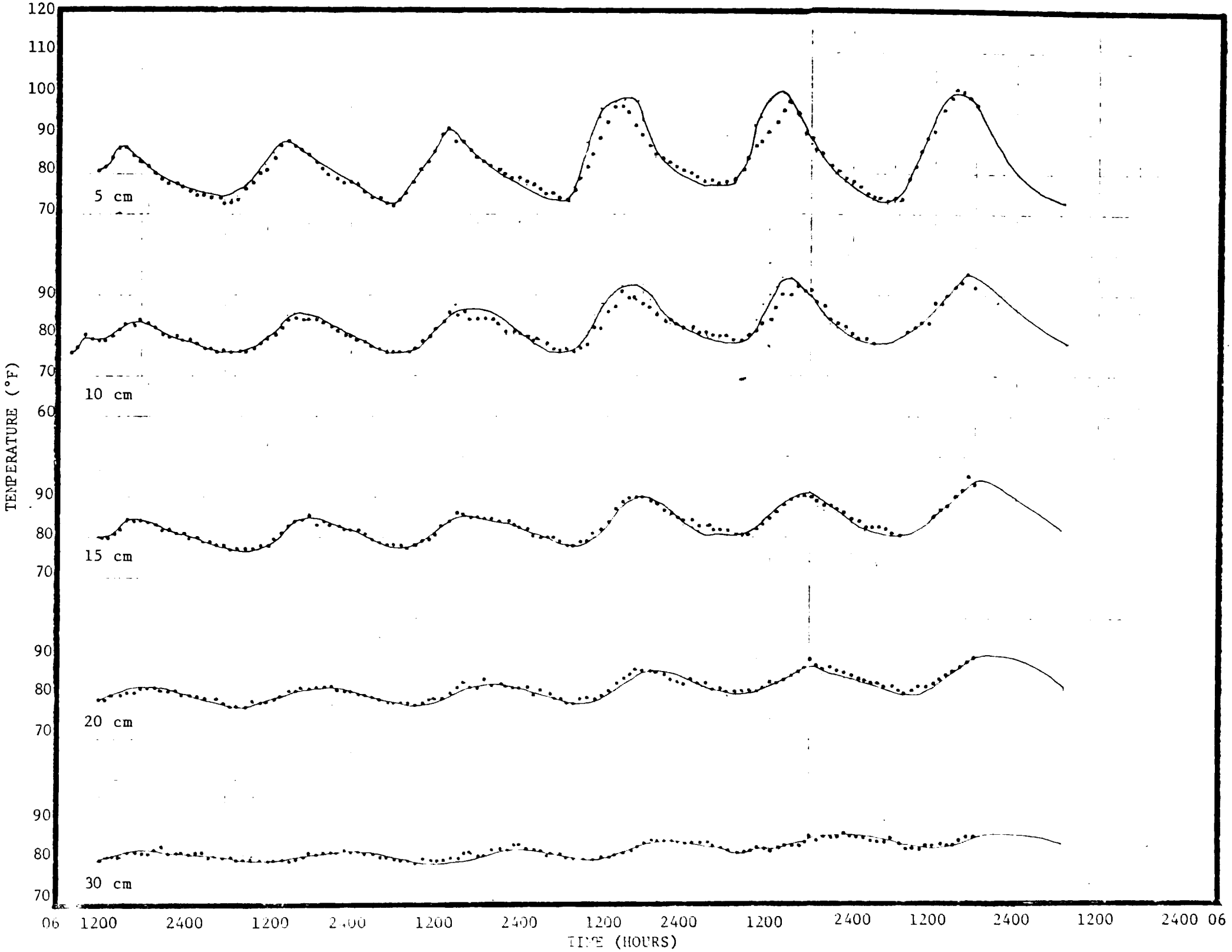


Figure 7. Actual (···) and Calculated (____) Soil Temperature Profiles for 0800 August 8 to 0700 August 15, 1970. Fun II, Plot II.

vegetation reduced the outgoing longwave radiation from the soil surface thus causing the surface temperature below the vegetation to cool at a slower rate than the bare soil.

Table 10 gives the total daily values of net radiation R, sensible heat flux G, and latent heat flux LE, for the soil beneath the 30 percent vegetation cover as calculated by the model. The measured average hourly values of cloud cover C, temperature T, wind speed U, relative humidity RH, and precipitation P, are the same as given previously in Table 9 for Plot I. A comparison of Table 9 and Table 10 shows the daily latent heat flux LE, for Plot II to be less than Plot I for August 8 and August 9, but becomes greater than Plot I for August 10-13. This is due to the large net radiation input for Plot I which essentially evaporated available moisture in a two day period. Plot II, due to the vegetative canopy, received a daily net radiation load of about 50 percent of the Plot I value; hence evaporation extended over a longer period of time. Figure 8 compares the simulated evaporation rates in millimeters (mm) of water per hour for Plot I and Plot II for the seven day period.

The total daily sensible heat flux remained negative for the first three days in Plot II and for only one day in Plot I. The net radiation was insufficient to supply the latent heat flux and soil heat flux in Plot I on August 8, therefore 4.2 langleys were drawn from the atmosphere. Thereafter, the evaporation rate declined rapidly and the net radiation provided an ample supply of energy for the energy balance process. Plot II maintained a negative sensible

Table 10. Total Daily Values in Langleys of Net Radiation R, Sensible Heat Flux H, Latent Heat Flux LE, and Soil Heat Flux G, for Run II, Plot II

| Date | Plot | R | H | LE | G |
|---|---|---|---|---|---|
| | II | | | | |
| 8/8/70 | | 127.5 | -31.7 | 197.1 | -37.9 |
| 8/9/70 | | 106.7 | -16.1 | 108.6 | 14.2 |
| 8/10/70 | | 62.9 | -9.6 | 46.5 | 16.0 |
| 8/11/70 | | 78.2 | 42.8 | 18.0 | 18.2 |
| 8/12/70 | | 4.9 | 13.1 | 1.0 | -9.2 |
| 8/13/70 | | 9.9 | 9.9 | 0.1 | -.1 |
| 8/14/70 | | 47.0 | 54.2 | 0.0 | -7.2 |

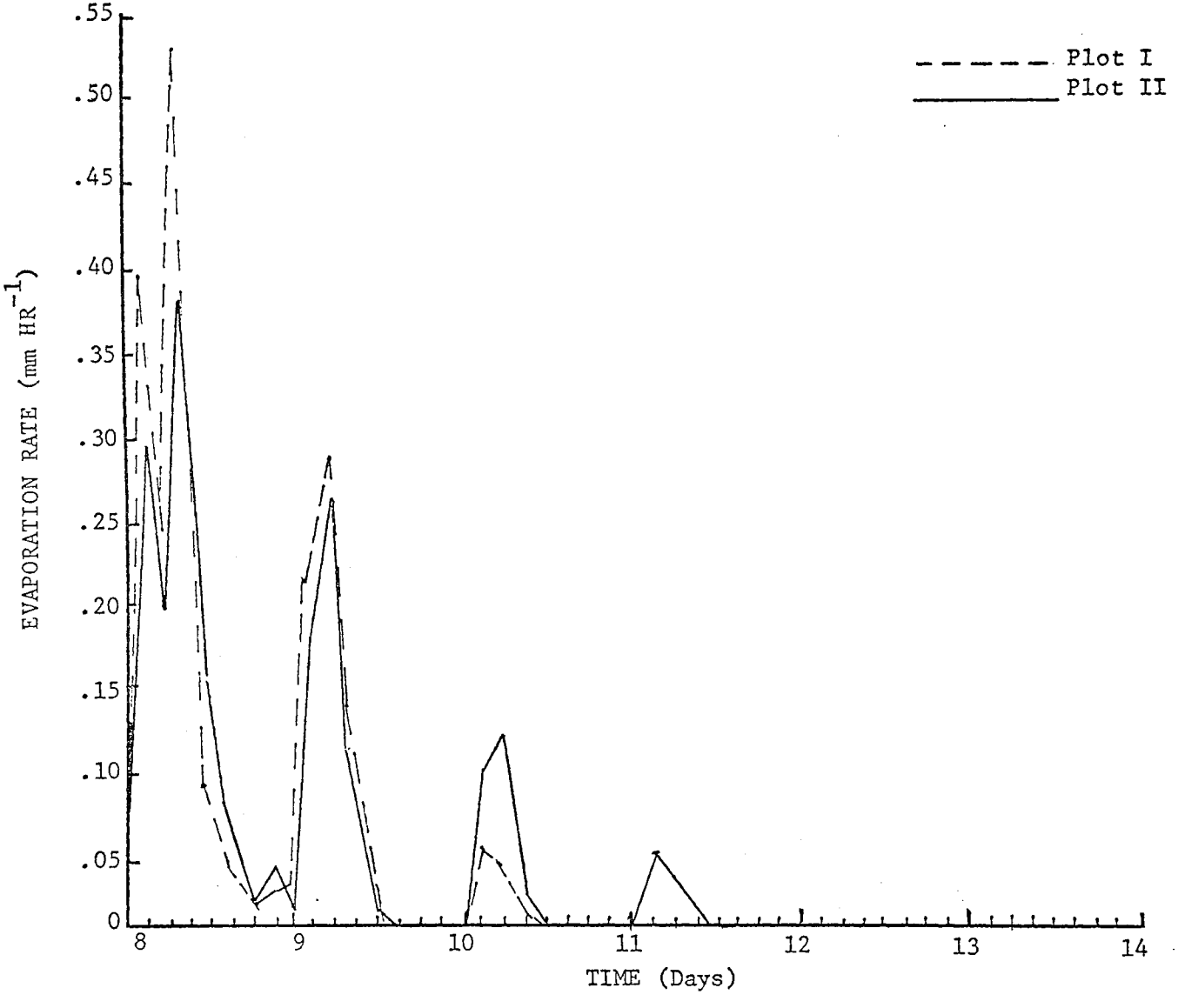


Figure 8. Comparison of Simulated Evaporation Rates for Plot I and Plot II

heat flux for August 8-10 because of the additional energy required to drive the latent heat flux than was provided by the net radiation.

## Run III--September 10-15, 1970

Plot I and Plot II were irrigated on the afternoon of September 9, 1970, and soil temperature monitoring began at 1700 September 9. The model was applied beginning 0800 September 10, 1970. The initial conditions used for the beginning of the period are shown in Table 11.

### Plot I

The initial soil moisture content for Plot I was 0.70 cm of water as shown in Table 11. Evaporation rates were very high the first day of the run period. A peak evaporation rate of 0.84 mm $hr^{-1}$ was reached at 1000, and the total evaporation for the 24 hour period 0800 September 10 to 0700 September 11 was 6.5 mm. The high evaporation rate for the time period was aided by a relatively high afternoon wind velocity of 4.4 m $sec^{-1}$. As shown in Table 12, the latent heat flux LE, accounted for 386 ly on September 10. The net radiation R, supplied 236 ly or 61 percent of the energy consumed in evaporation. The additional energy input came from the warm air layer over the plot and from the soil column itself. Table 12 also shows a steady decline in the net radiation with time as the soil dries and the surface temperature increases. The exception occurs September 12, 1970 and is due to an increase in cloud cover for the day.

The sensible heat flux H, increased rapidly on September 10 and September 11 as the evaporation rate declines. The sensible heat

Table 11. Initial Conditions for Plot I and Plot II (September 10-15, 1970)

| Symbol | Magnitude | | Units |
|---|---|---|---|
| | Plot I | Plot II | |
| $W_{sl}$ | 0.70 | 0.75 | cm |
| $W_{sk}$ | 0.50 | 0.50 | cm |
| $W_{pl}$ | | 3.00 | cm |
| $W_{pk}$ | | 1.00 | cm |
| $T_{sl}$ | 90.0 | | °F |
| $\bar{T}_s$ | 85.0 | | °F |
| $T_{pl}$ | | 82.0 | °F |
| $\bar{T}_p$ | | 82.0 | °F |
| $Z_{op}$ | | 6.0 | cm |
| $Z_{os}$ | 1.0 | | cm |

Table 12. Total Daily Values in Langleys of Net Radiation R, Sensible Heat Flux H, Latent Heat Flux LE, Soil Heat Flux G, and Average Hourly Cloud Cover N (Tenths), Air Temperature T (°F), Wind Speed U ($m\ sec^{-1}$), Relative Humidity RH (Percent), and Precipitation P (mm), for Run III, Plot I.

| Date | Plot | R | H | LE | G | N | T | U | RH | P |
|---|---|---|---|---|---|---|---|---|---|---|
| | I | | | | | | | | | |
| 9/10/70 | | 236.4 | -72.3 | 386.0 | -77.2 | 2.3 | 84.0 | 2.4 | 49.5 | 0.0 |
| 9/11/70 | | 170.0 | 90.3 | 16.8 | 62.9 | 1.4 | 82.5 | 0.8 | 56.3 | 0.0 |
| 9/12/70 | | 138.7 | 139.9 | 3.1 | -4.3 | 3.2 | 77.7 | 1.6 | 67.8 | 0.0 |
| 9/13/70 | | 176.9 | 170.8 | 0.1 | 6.0 | 0.8 | 79.1 | 1.8 | 60.1 | 0.0 |
| 9/14/70 | | 167.0 | 191.8 | 0.0 | -31.2 | 0.0 | 72.4 | 1.7 | 45.2 | 0.0 |
| 9/15/70 | | 137.1 | 124.3 | 0.0 | 12.8 | 0.0 | 72.9 | 1.0 | 41.5 | 0.0 |

flux on September 14 and September 15 appears to be influenced by wind speed. At this time evaporation has ceased and no cloud cover was recorded.

Figure 9 shows the hourly simulated energy balance for September 12, 1970. As seen from the figure the net radiation R, fluctuated greatly from 1100 to 1800. The soil heat flux G, was positive from 0800 to 1600 at which time it became negative. The soil heat flux closely followed the net radiation. Sensible heat flux was positive from 0800 to 2000 indicating much of the net radiation absorbed at the surface was used to warm the air layer above the plot. The latent heat flux was essentially zero for the 24 hour period.

Figure 10 shows the actual versus calculated soil temperature variation for the test period. The peak temperature on September 10 at 5 cm was approximately 12°F less than for the same time September 11. This is due to the large amount of radiation used in the evaporation process on September 10. The peak temperature on September 12 at 5 cm was 8°F less than the calculated temperature for this time period. A check of the cloud cover N, at this time revealed 5 tenths coverage at the airport, however N over the plots for the same time may have actually been greater than 5 tenths thus accounting for a lower actual soil temperature than the model calculated.

Plot II

Figure 11 shows the actual versus calculated soil temperature variation beneath a 40 percent plant cover. Again, as previously discussed in Run II, the most apparent result, when comparing the

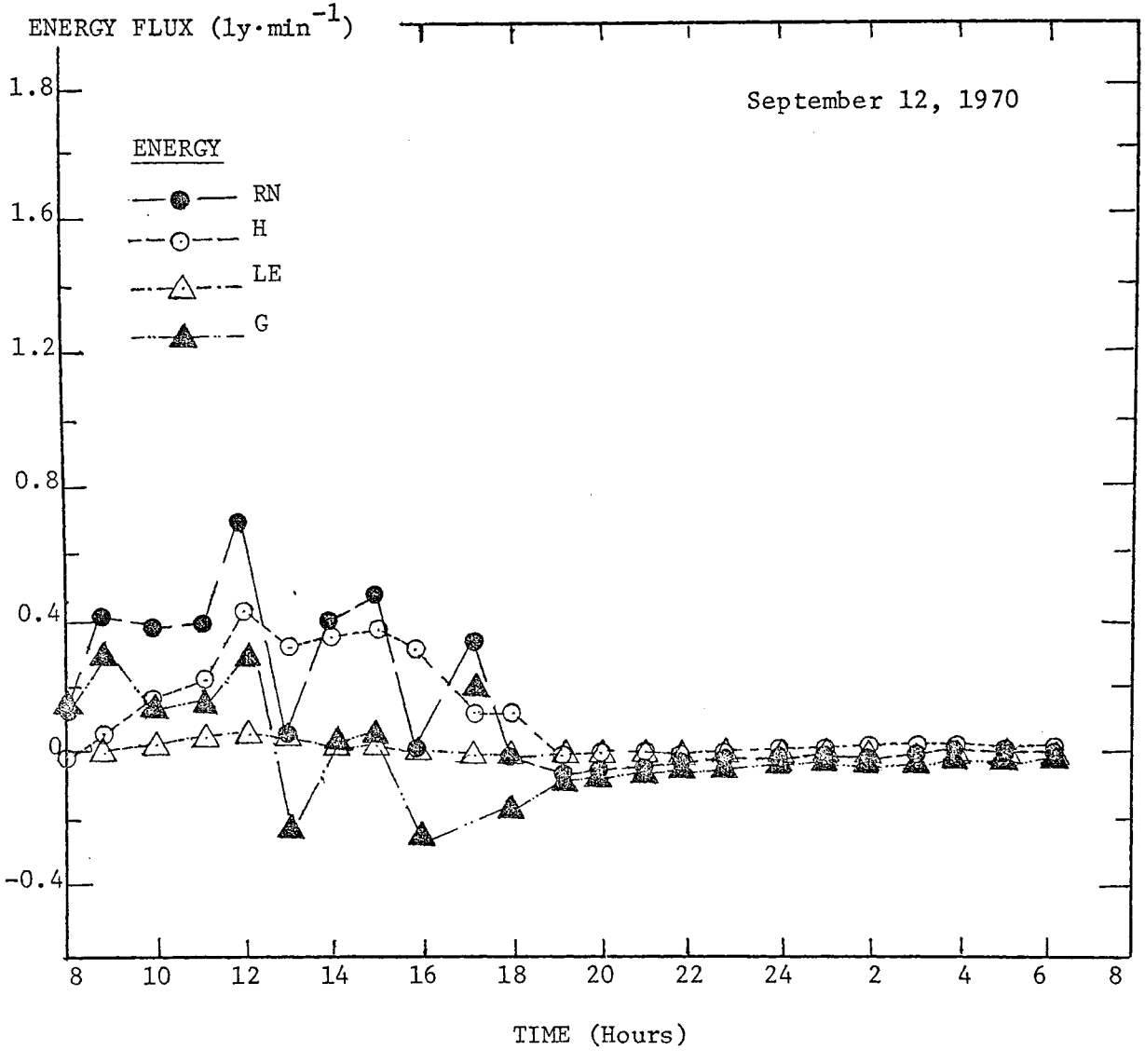


Figure 9. Hourly Values of Simulated Energy Balance for September 12, 1970

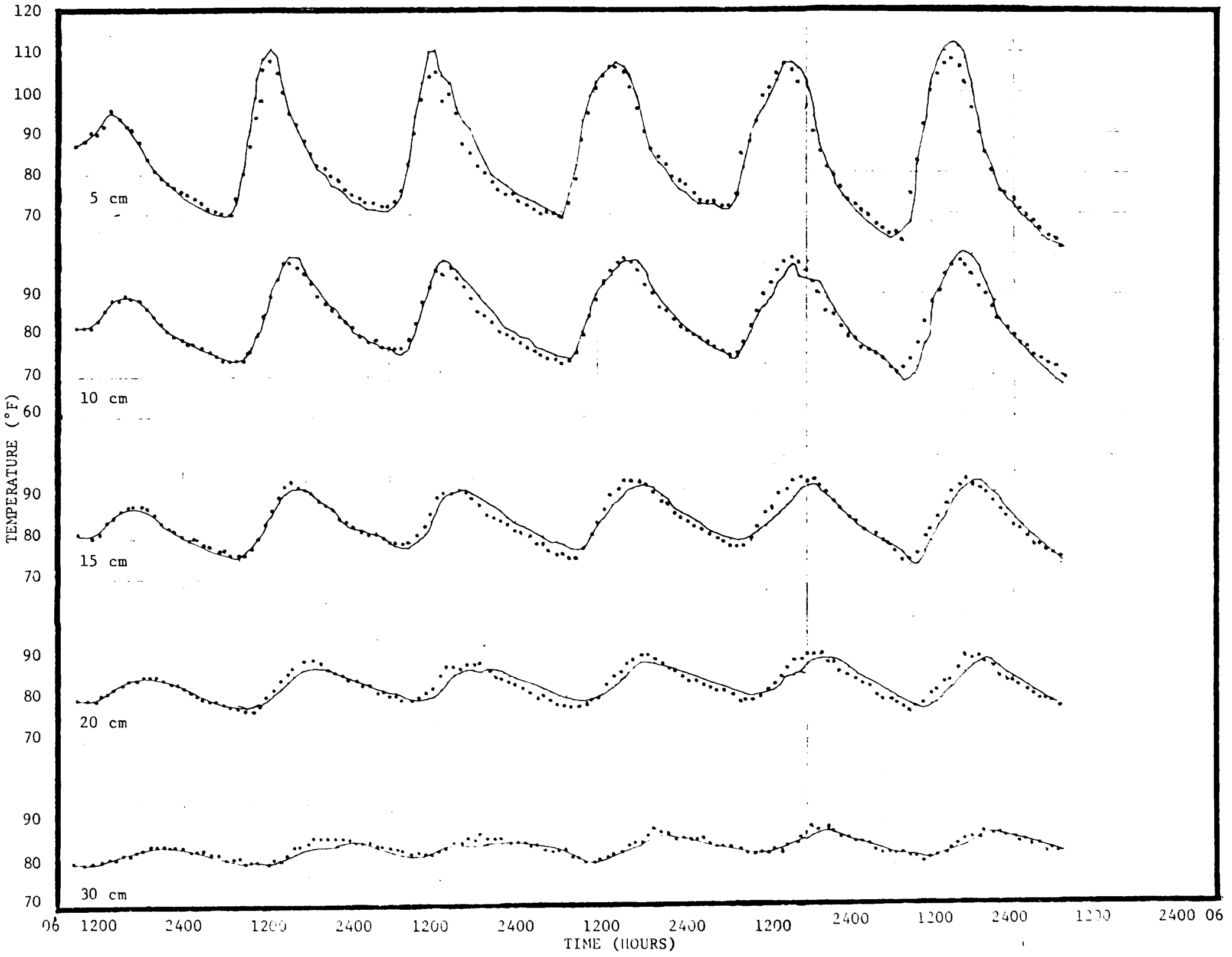


Figure 10. Actual (···) and Calculated (——) Soil Temperature Profiles for 0800 September 10 to 0700 September 16, 1970. Run III, Plot I.

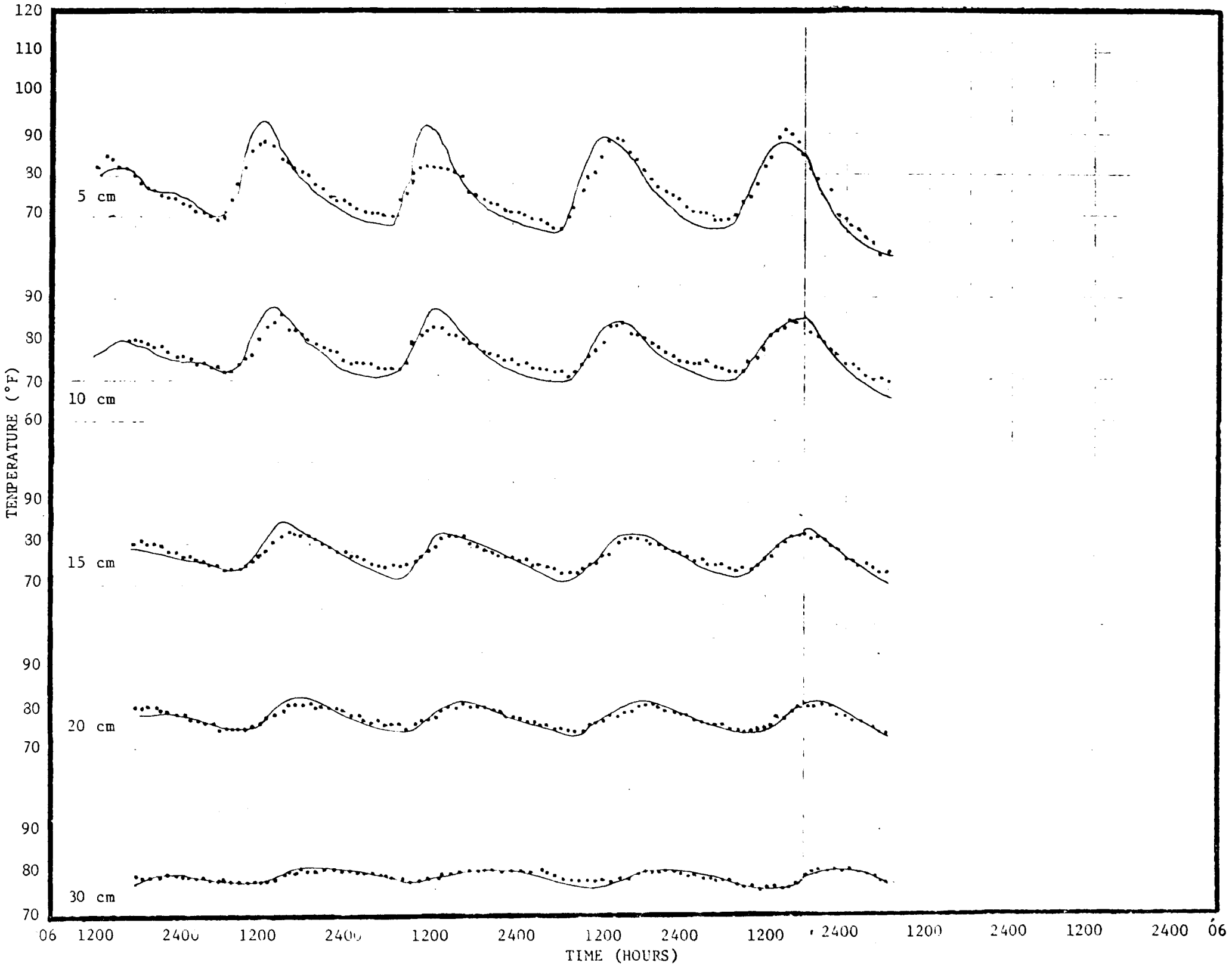


Figure 11. Actual (···) and Calculated (___) Soil Temperature Profiles for 0800 September 10 to 0700 September 16, 1970. Run III, Plot II.

temperature variation of Plot I and Plot II, was the temperature damping effect beneath the plant canopy. The peak temperature at 5 cm in Plot I for the entire test period was approximately 10 °F higher than for Plot II. The minimum temperature at all depths in Plot II however, was consistently lower than the minimum temperature at all depths in Plot I for September 12-15. This is due to a prolonged evaporation period in Plot II caused by a reduced radiation load.

The most noticeable discrepancy in the actual and calculated soil temperature occurs from 1000 to 1600 September 12. As seen from Figure 11, the maximum temperature at 5 cm on that date was approximately 4 °F to 6 °F less than the maximum temperature at 5 cm on September 11 and September 13. A check of cloud cover conditions over that time period revealed an average cloud cover of 66 percent. A possible cause for the discrepancy could lie in the pyrheliometer correction factor. The correction factor was determined on clear days, therefore when the factor was applied to a 7 hour span of cloudy weather, the incoming solar radiation may have been overestimated. September 12, 1970 was the only day during the run experiencing cloud cover in excess of 8 tenths for the period mentioned.

Table 13 gives the total daily values of net radiation R, sensible heat flux H, soil heat flux G, and latent heat flux LE, for Plot II as calculated by the model. The measured average hourly values of cloud cover C, temperature T, wind speed U, relative humidity RH, and precipitation P, are the same as given previously in Table 12.

Table 13. Total Daily Values in Langleys of Net Radiation R, Sensible Heat Flux H, Latent Heat Flux LE, and Soil Heat Flux G, for Run III, Plot II

| Date | Plot | R | H | LE | G |
|---|---|---|---|---|---|
| | II | | | | |
| 9/10/70 | | 177.0 | 153.8 | 393.3 | -62.5 |
| 9/11/70 | | 102.0 | 58.0 | 24.0 | 20.0 |
| 9/12/70 | | 30.3 | 15.3 | 10.0 | 5.0 |
| 9/13/70 | | 79.6 | 64.0 | 4.0 | 11.6 |
| 9/14/70 | | 68.0 | 40.0 | 3.0 | 25.0 |
| 9/15/70 | | 29.7 | 30.1 | 0.0 | -0.4 |

A comparison of Table 12 and Table 13 shows the latent heat flux LE, for September 10, 1970 to be greater for Plot II than for Plot I. Although the opposite might be expected, the greater evaporation rate of the soil beneath the plant canopy was due to two factors: 1) the greater roughness length of the canopy and hence increased turbulence, and 2) a relatively high average wind speed for the day of 2.4 m $sec^{-1}$. The latent heat flux decreased greatly on September 11, 1970. This is due to a combination of factors including a decrease in wind speed, a slight drop in ambient air temperature, and an increase in relative humidity.

# CONCLUSIONS

The model analysis compared favorably with the field data, and the three experimental runs prove the utility of model simulation for determining soil temperature profiles. Departures of the actual and calculated temperatures can in most cases be attributed to the single variable cloud cover.

Additional uses of the model may be to determine soil temperature profiles over large spatial areas assuming the soil moisture content is essentially uniform at the beginning of the trial period. Also the model may be used to simulate changes in the soil temperature profile based on artificial manipulation of the input parameters. The model's ability as a predictive tool lies in the capability to know in advance values of the input parameters; however, in arid areas of the globe where cloud cover is minimal, the daily variation of incoming radiation, air temperature, windspeed, and relative humidity may be essentially the same. Value of the model stems not only from its capability to simulate soil temperature profiles, but also from its ability to simulate the energy balance at the earth's surface.

The results of the model's performance can be judged only by its ability to simulate the soil's temperature profile. The equations used for the energy balance simulation appear to give a reasonable representation of the physical processes occurring at the earth/air interface, however, to substantiate the fluxes and net radiation calculated, the model would require additional instrumentation. Additional study would be merited into the model's use as a method for calculating soil evaporation and evapotranspiration from plants.

# APPENDIX A

## MODIFICATION OF SURFACE ENERGY BALANCE

The introduction of a plant canopy over a soil surface results in a partitioning of energy between the plant canopy and the soil surface, thus an energy balance equation must be written for both and solved simultaneously.

The plant energy balance will be solved initially. The two stages of evapotranspiration are a = 1 and a = $w/w_{kp}$ as for the bare soil case.

### Plant Energy Balance

The energy balance of the plant canopy may be expressed as

$$Gp = (-LEp + I\downarrow - 2I\uparrow p + I\uparrow s)(1 - \tau I) + Q(1 - \alpha p)(1 - \tau) + Hs - Hp \quad (1)$$

where

Gp = the plant heat storage rate

LEp = the plant latent heat flux rate

I↓ = the counter radiation from the atmosphere

I↑p = the longwave radiation from the plant surface

I↑s = the longwave radiation from the soil surface

αp = the plant albedo

Hp = the sensible heat flux from the plant surface

Hs = the sensible heat flux from the soil surface

$\tau$ = the amount of ground receiving solar radiation depending on the sun angle ($\tau=\tau I \cos z$, where z = zenith angle)

The percentage of soil surface beneath the plant canopy receiving solar radiation $\tau$, is approximated by $\tau I \cos z$ where $\tau I$ is the amount of ground cover in percent and z is the zenith angle. Figure 1A shows a sun-path diagram for Tucson, Arizona from which the zenith angle for any hour of the day and month of the year may be determined.

The energy balance of the plant is compromised of heating by the absorption of longwave counter radiation $I\downarrow$, the absorption of longwave radiation from the soil survace $I\uparrow s$, the absorption of incoming solar radiation $Q(1 - \alpha p)$, and the absorption of sensible heat from the soil surface Hs. Cooling occurs by the latent heat of evapotranspiration LEp, emission of longwave radiation $I\uparrow p$, and the transfer of sensible heat to the atmosphere Hp. Equation (1) must be solved for known variables and $\Delta T_p$.

Radiation Components

The radiation components of Equation (1) are given by

$$(I\downarrow - 2I\uparrow p + I\uparrow s)(1 - \tau I) + Q(1 - \alpha p)(1 - \tau) \qquad (2)$$

The counter radiation I, can be defined as

$$I\downarrow = I\uparrow p - I \qquad (3)$$

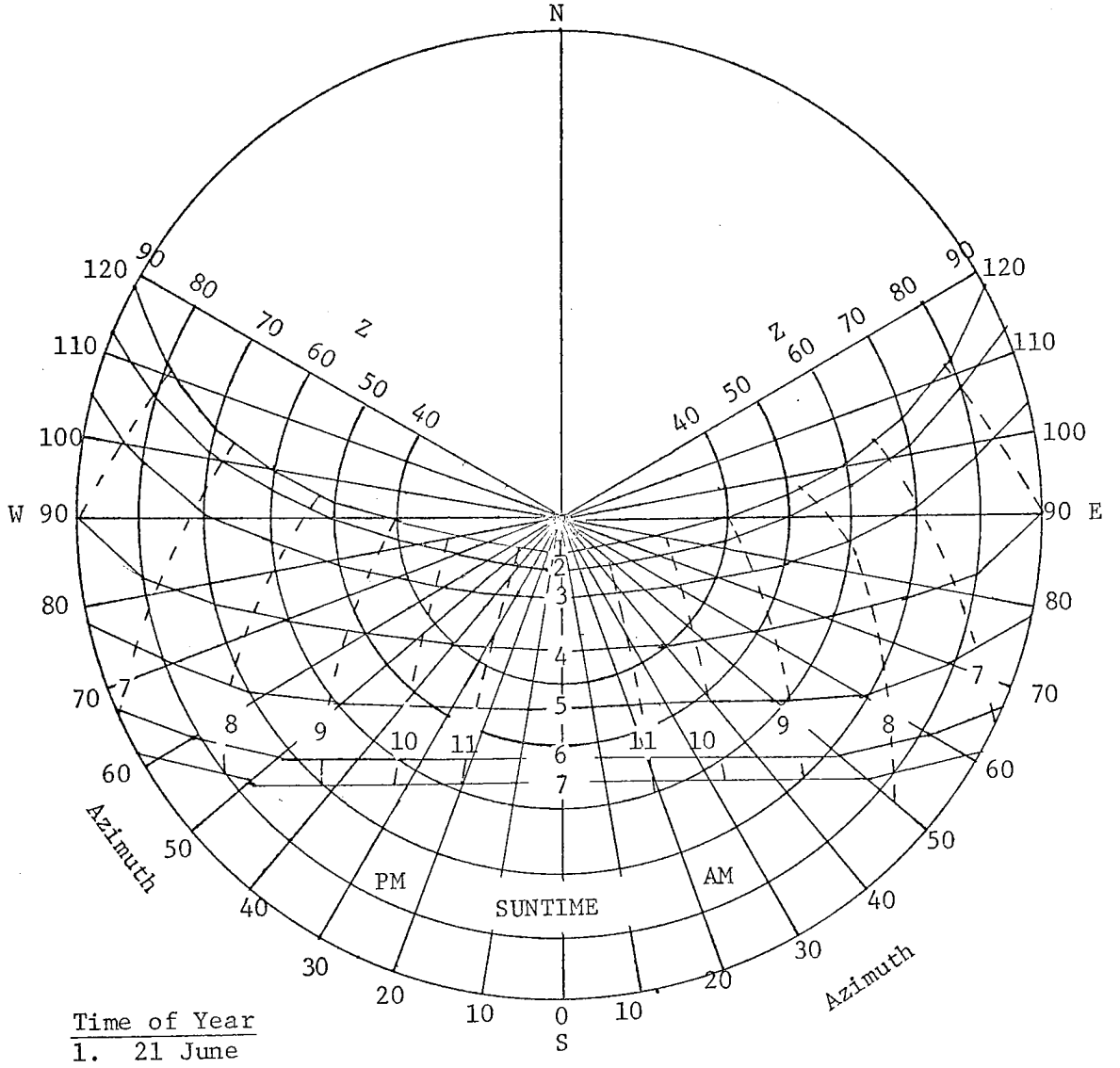


Figure A-1. Sun-Path Diagram for Tucson

where

I = the effective outgoing radiation

Rearranging Equation (3) yields $I\downarrow - I\uparrow p = -I$. This is simply the negative of the effective outgoing radiation as given in Equation (3). The longwave radiation emitted by the plant $I\uparrow p$, is given by the Stefan-Boltzmann law

$$I\uparrow p = \varepsilon p \sigma T_p^4 \tag{4}$$

where

$\varepsilon p$ = the plant emissivity

$T_p$ = the plant temperature

In order to get Equation (4) into a form involving $\Delta T$ , $\varepsilon p \sigma T^4$ is added and subtracted from Equation (4) giving

$$I\uparrow p = \varepsilon p \sigma T_p^4 + \varepsilon p \sigma T^4 - \varepsilon p \sigma T^4 \tag{5}$$

or

$$I\uparrow p = 4\varepsilon p \sigma T^3 \Delta T_p + \varepsilon p \sigma T^4 \text{ or } a3 \Delta T_p + \varepsilon p \sigma T^4 \tag{6}$$

The heat flux from the soil surface $I\uparrow s$, can also be given by the Stefan-Boltzmann law

$$I\uparrow s = \varepsilon s \sigma T_s^4 \tag{7}$$

or

$$\begin{aligned} I\uparrow s &= 4\varepsilon s \sigma T^3 \Delta T_s + \varepsilon s \sigma T^4 \\ &= a3' \Delta T_s + \varepsilon s \sigma T^4 \end{aligned} \tag{8}$$

where

$a3' = \varepsilon s a3 / \varepsilon p$

If Equation (2) is rewritten as

$$(I\downarrow - I\uparrow p - I\uparrow p + I\uparrow s)(1 - \tau I) + Q(1 - \alpha p)(1 - \tau) \qquad (9)$$

then the equation becomes

$$(-I - I\uparrow p + I\uparrow s)(1 - \tau I) + Q(1 - \alpha p)(1 - \tau) \qquad (10)$$

or

$$(-a2 - a3\ \Delta T_p - a3\ \Delta T_p + a3'\ \Delta T_s + (\varepsilon s - \varepsilon p)\ \sigma T^4)(1 - \tau I) + a1(1 - \alpha p)(1 - \tau) \qquad (11)$$

Sensible Heat Hs, Hp

The aerodynamic equation given previously in Equation (19) under Model Derivation applies for both Hs and Hp. The sensible heat flux from the plant surface is given by

$$Hp = \frac{pCpDp(T_p - T)}{RT} \qquad (12)$$

where

Hp = the sensible heat flux from the plant surface

Dp = the plant transfer coefficient

The transfer coefficient Dp, is calculated in the same manner as the coefficient for the bare soil. The roughness length $Z_{op}$, was obtained from Sellers (1965b, Table 20, p. 150). Equation (12) may be written as $a4\Delta T_p$.

The sensible heat emitted from the soil surface that warms the plant is given by

$$Hs = \frac{pCpD(\Delta T_s - \Delta T_p)}{RT} \qquad (13)$$

The term $\Delta T_s - \Delta T_p$ is equal to $T_p - T_s$.

Latent Heat Flux LEp

Case I a = 1:

The latent heat flux LEp, given previously in Equation (21) is again used with minor modifications. The finite difference of the Claussius-Claypeyron equation is

$$(es - esa) = \frac{0.622\ Lesa\ (T_p - T)}{RT^2} \tag{14}$$

Again adding and subtracting the vapor pressure of the air at temperature T, gives

$$es - esa + ez - ez = \phi\ T_p \tag{15}$$

Substitution of Equation (15) into Equation (21) gives

$$LEp = \frac{0.622LDp}{RT}\ [\phi(T_p - T) + (esa - e)] \tag{16}$$

Equation (16) can be written as $a5\Delta T_p + a6$ where

$$a5 = \frac{0.622LDp\ \Delta T_p}{RT}\ \phi \text{ and } a6 = \frac{0.622LDp}{RT}\ (esa - e) \tag{17}$$

Case II $a = w/w_{kp}$:

The final form of the aerodynamic equation is similar to Equation (32) in the bare soil model and is given by

$$LEp = \frac{w_{p1}(a5\Delta T_p + a6}{a12\Delta T_p - a11} \tag{18}$$

or

$$LEp = \frac{a10\Delta T_p + a9}{a12\Delta T_p + a11} \tag{19}$$

where

$$a9 = a6w_{p1}$$

$$a10 = a5w_{p1}$$

$$a11 = w_{kp} + \frac{0.311Dp(esa - e)}{RT}$$

$$a12 = \frac{0.311Dp\phi}{RT}$$

Plant Heat Storage Rate Gp

The heat flux in the plant is solved in the same manner as heat flux in the soil model. The final solution for the plant heat flux is given by

$$Gp = [187.45(C\lambda)^{1/2}]\ \Delta T_p + 21.71(C\lambda)^{1/2}\ [T - \bar{T}_p + 2/\omega\ (T - T_{p1})] \tag{20}$$

where

$(C\lambda)^{1/2}$ = the thermal property of the plant

$\bar{T}_p$ = the plants previous 24 hour average temperature

$T_{p1}$ = the previous hours plant surface temperature

All components for Equation (1) have now been defined in terms of known variables and $\Delta T_s$ and $\Delta T_p$. Substituting the form of the equations in $a_i$, $\Delta T_s$, and $\Delta T_p$ back into Equation (1) yields

$$a7\ \Delta T_p + a8 = (1 - \tau I)(-a5\ \Delta T_p - a6 - a2 - 2a3\ \Delta T_p + (\varepsilon s - \varepsilon p)\ T^4 + a3'\ \Delta T_s) + a4'\ \Delta T_s + a1(1 - \tau) - a4'\ \Delta T_p - a4\ \Delta T_p \tag{21}$$

Collecting terms yields

$$[a4' + a4 + a7\ (a5 + 2a3)(1 - \tau I)]\ \Delta T_p = [a4' + a3'\ (1 - \tau I)]\ \Delta T_s + [(\varepsilon s - Gp)\ T^4 + a1(1 - \tau) - (a2 + a6)(1 - \tau I) - a8] \tag{22}$$

If new variables b1, b2, and b3 are defined, then Equation (22) reduces to the linear equation

$$b1\Delta T_p = b2\Delta T_s + b3 \tag{23}$$

for Case I where

$$b1 = a4' + a4 + a7 + (a5 + 2a3)(1 - \tau I)$$

$$b2 = a4' + a3'(1 - \tau I)$$

$$b3 = (\varepsilon s - \varepsilon p)\sigma T^4 + a1(1 - \tau) - (a2 + a6)(1 - \tau I) - a8$$

For Case II, Equation (23) becomes

$$b1\Delta T_p = b2\Delta T_s + b3 + a5\Delta T_p + a6 - \frac{a10\Delta T_p + a9}{a12\Delta T_p + a11}\ (1 - \tau I) \tag{24}$$

Again collecting terms, Equation (24) becomes

$$[(b1 - a5)\ \Delta T_p + (-a6 - b3 - b2\Delta T_s)](a12\Delta T_p + a11) = -a10\Delta T_p - a9 \tag{25}$$

where

$$b1 = b1/(1 - \tau I)$$

$$b2 = b2/(1 - \tau I)$$

$$b3 = b3/(1 - \tau I)$$

Expanding Equation (25) and again collecting terms yields

$$a12(b1 - a5)\Delta T_p^2 + [-a12(a6 + b3) + a11(b1 - a5) + a10]\,\Delta T_p - a12b2\Delta T_s\Delta T_p - a11b2\Delta T_s - a11(ab + b3) + a9 = 0 \quad (26)$$

If

$$b4 = a12(b1 - a5)$$

$$b5 = - a12(a6 + b3) + a11(b1 - a5) + a10$$

$$b6 = - a12b2$$

$$b7 = - a11b2$$

$$b8 = - a11(a6 + b3) + a9$$

then Equation (26) may be reduced to the quadratic equation

$$64\Delta T_p^2 + b5\Delta T_p + b6\Delta T_s\Delta T_p + b7\Delta T_s + b8 = 0 \quad (27)$$

## Soil Energy Balance

The energy balance of the soil beneath a plant canopy can be written as

$$Gs = -LEs - Hs + \tau Q(1 - \alpha s) + I{\downarrow}p\ (1 - \tau I) + I{\downarrow}\tau I - I{\uparrow}s \quad (28)$$

where

Gs = the soil heat flux

LEs = the soil latent heat flux

The net rate Gs at which the heat content of the soil column is changing is equal to the sum of the rates at which heat is being added by incoming short wave radiation $Q(1 - \alpha s)$, incoming longwave counter radiation from the atmosphere $I{\downarrow}\tau I$, and longwave radiation radiated

downward from the plant $I\downarrow p\tau I$, minus the rate at which heat is being lost by evaporation LEs, sensible heat flux Hs, and the emission of longwave radiation from the soil surface $I\uparrow s$.

Radiation Components

The radiation components of Equation (28) are given by

$$\tau Q(1 - \alpha s) + I\downarrow p\ (1 - \tau I) + I\downarrow \tau I - I\uparrow s \tag{29}$$

where

$\tau Q(1-\alpha s)$ = the amount of incoming solar radiation absorbed at the soil surface

$I\downarrow p$ = the longwave radiation emitted by the plant

$I\downarrow$ = the atmospheric counter radiation

$I\uparrow s$ = the longwave radiation emitted by the soil

The longwave radiation from the plant $I\downarrow p$, is given by

$$\varepsilon p\sigma T^4 + 4\varepsilon p\sigma T^3 \Delta T_p \tag{30}$$

or $a3\Delta T_p + \varepsilon p\sigma T^4$.

The negative outgoing radiation is defined to be $I\downarrow - I\uparrow p = -I$. If $I\downarrow p$ is added to both sides of Equation (3), the equation becomes

$$I\downarrow - I\uparrow p + I\downarrow p = -I + I\downarrow p \tag{31}$$

which is the effective outgoing radiation.

Assuming the plant radiates equally both up and down, the long radiation emitted downward is given by

$$I\downarrow p = 4\varepsilon p\sigma T^3 \Delta T_p + \varepsilon p\sigma T^4 \tag{32}$$

thus Equation (32) becomes $-a2 + a3\Delta T_p + \varepsilon p\sigma T^4$.

The longwave radiation emitted from the soil is given by

$$I\uparrow s = 4\varepsilon s\sigma T^3\Delta T_s + \varepsilon s\sigma T^4 \tag{33}$$

If a3' is defined as εs a3/εp, then Equation (33) can be written as $a3'\Delta T_s + \varepsilon s\sigma T^4$.

The longwave radiation components of Equation (29) can now be rewritten as

$$(a3\Delta T_p + \varepsilon p\sigma T^4)(1 - \tau I) + (-a2 + a3\Delta T_p + \varepsilon p\tau T^4)\ \tau I - (a3'\Delta T_s + \varepsilon s\sigma T^4) \tag{34}$$

Sensible Heat Hs

The sensible heat flux Hs, is given by

$$Hs = \frac{p\ Cp\ Dm}{RT}(\Delta T_s - \Delta T_p) \tag{35}$$

or $a4'(\Delta T_s - \Delta T_p)$ where a4' is equal to Dm a4/Dp.

Latent Heat Flux LEs

Case I a = 1:

The equation for the latent heat flux is derived as before and has a final form of

$$LEs = a5'\Delta T_s - a5'\Delta T_p + a6' \tag{36}$$

where

a5' = Dm a5/Dp

a6' = Dm a6/Dp

Case II $a = w/w_{ks}$:

The latent heat flux for Case II is given by

$$LEs = \frac{a10'\Delta T_s - a10'\Delta T_p + a9'}{a12\Delta T_s - a12\Delta T_p + a11'} \tag{37}$$

where

$$a9' = a6\ w_{s1}$$

$$a10' = a5\ w_{s1}$$

$$a11' = w_{ks} + 0.311\ \frac{Dm}{RT}\ (esa - e)$$

The above equation is similar to Equation (19) for the latent heat flux from the plant canopy. The $\Delta T_p$ term was replaced by $\Delta T_s - \Delta T_p$ and the appropriate initial soil moisture content $w_{s1}$, and transfer coefficient Dm, were included.

Soil Heat Flux Gs

The equation for soil heat flux given previously in Equation (42) of Model Derivation is again applicable. The equation is given by

$$a7'\Delta T_s + a8' \tag{38}$$

where

$$a7' = 187.545\ (C\lambda)^{1/2}$$

$$a8' = 21.708\ (C\lambda)^{1/2}\ [T_a - \bar{T}_s + 7.6394\ (T_a - T_{s1})]$$

All components for Equation (28) have now been defined in terms of known variables and $\Delta T_s$ and $\Delta T_p$. Substituting the form of the equations in ai, ai', $\Delta T_s$, and $\Delta T_p$ into Equation (28) yields for Case I

$$a7'\Delta T_s + a8' = a5'\Delta T_p - a6' - a4'(\Delta T_s - \Delta T_p) + a1' + (a3\Delta T_p + \varepsilon p\sigma T^4)(1 - \tau I) - a5'\Delta T_s + (a3\Delta T_p + \varepsilon p\sigma T^4 - a2 - a3\Delta T_p)\tau I - a3'\Delta T_s - \varepsilon s\sigma T^4 \quad (39)$$

Collecting terms yields

$$(a5' + a7' + a4' + a3')\Delta T_s = [a4' + a5' + a3(1 - \tau I)]\Delta T_p + [a1' - a6' - a8' - (\varepsilon s - \varepsilon p)\sigma T^4 - a2\tau I] \quad (40)$$

If new variables b1', b2', and b3' are defined, then Equation (40) reduces to the linear equation

$$b1'\Delta T_s - b2'\Delta T_p + b3' \quad (41)$$

where

$$b1' = a7' + a4' + a3' + a5'$$

$$b2' = a4' + a5' + a3(1 - \tau I)$$

$$b3' = a1' - a6' - a8' - (\varepsilon s - \varepsilon p)\sigma T^4 - a2\tau I$$

For Case II Equation (41) becomes

$$b1'\Delta T_s = b2'\Delta T_p + b3' - a5'\Delta T_p + a6' + a5'\Delta T_s - \frac{a10'\Delta T_s - a10'\Delta T_p + a9'}{a12\Delta T_s - a12\Delta T_p + a11'} \quad (42)$$

Again collecting terms, Equation (42) becomes

$$a12(b2' - 2a5') + b1')\Delta T_p\Delta T_s + a12(a5' - b1')\Delta T_s^2 + [a12(b3' + b6') - a10' + a11'(a5' - b1')]\Delta T_s - a12(b2' - a5')\Delta T_p^2 + [a11'(b2' - a5') + a10' - a12(b3' + a6')]\Delta T_p + a11'(b3' + a6' - a9') = 0 \quad (43)$$

If

$$b9 = a12(a5' - b1')$$

$$b10 = a12(b3' + b6') - a10' + a11'(a5' - b1')$$

$$b11 = -a12(b2' - a5')$$

$$b12 = a11'(b2' - a5') + a10' - a12(b3' + a6')$$

$$b13 = a12(b2' - 2a5' + b1')$$

$$b14 = a11'(b3' + a6') - a9'$$

then Equation (43) may be reduced to the quadratic form

$$b9\Delta T_s^2 + b10\Delta T_s + b11\Delta T_p^2 + b12\Delta T_p + b13\Delta T_s\Delta T_p + b14 = 0 \qquad (44)$$

The final equations of the soil and plant energy balance for Case I and Case II may now be solved for three unique cases $w_s \geq w_{ks}$, $w_p \geq w_{kp}$; $w_s < w_{ks}$, $w_p \geq w_{kp}$; and $w_s < w_{ks}$, $w_p < w_{kp}$.

Solution I $w_s \geq w_{ks}$, $w_p \geq w_{kp}$

The two final equations satisfying the above conditions are Equation (23) and Equation (41). Rewritting the two equations

$$b1\Delta T_p - b3 - b2\Delta T_s = 0$$

$$b2'\Delta T_p + b3' - b1'\Delta T_s = 0$$

yields two linear equations and two unknowns which may be solved simultaneously. The final solution for $T_p$ and $T_s$, respectively, is given by

$$\Delta T_p = \frac{b2b3' + b1'b3}{b1b1' - b2b2'} \qquad (45)$$

and

$$\Delta T_s = \frac{b2'\Delta T_p + b3'}{b1'} \qquad (46)$$

Equation (45) is solved initially for $\Delta T_p$ and that result is then substituted into Equation (46) to determine $\Delta T_s$.

Solution II $w_s < w_{ks}$, $w_p \geq w_{kp}$

The two final equations satisfying the above conditions are Equation (23) and Equation (44). Rewriting the two equations

$$b1\Delta T_p - b2\Delta T_s - b3 = 0$$

$$b9\Delta T_s^2 + b10\Delta T_s + b11\Delta T_p^2 + b12\Delta T_p + b13\Delta T_s\Delta T_p + b14 = 0$$

yields a linear and a quadratic equation in the two desired unknowns $\Delta T_s$ and $\Delta T_p$. If the first equation is substituted into the second equation, the form becomes

$$b9\Delta T_s^2 + b10\Delta T_s + \frac{b11}{b1^2}(b2^2\Delta T_s^2 + 2b2b3\Delta T_s + b3^2) + \frac{b12}{b1}(b5\Delta T_s + b3) + \frac{b13}{b1}(b2\Delta T_s^2 + b3\Delta T_s) + b14 = 0 \qquad (47)$$

If new variables b15, b16, and b17 are defined, then Equation (47) may be reduced to

$$\Delta T_s = \frac{-b16 \pm (b16^2 - 4b15b17)^{1/2}}{2b15} \qquad (48)$$

where

$$b15 = b9 + b11\frac{(b2)^2}{b1} + b13\frac{(b2)}{b1}$$

$$b16 = b10 + 2\frac{(b2b3b11)}{b1^2} + b12\frac{(b2)}{b1} + b13\frac{(b3)}{b1}$$

$$b17 = b11\frac{(b3)^2}{b1} + b12\frac{(b3)}{b1} + b14$$

Equation (23) is then solved as before giving

$$\Delta T_p = \frac{(b2\Delta T_s + b3)}{b1} \qquad (49)$$

Solution III $w_s > w_{ks}$, $w_p > w_{kp}$

The two final equations satisfying the above conditions are given by Equation (27) and Equation (44). Rewriting the two equations

$$b4\Delta T_p^2 + (b5 + b6\Delta T_s)\Delta T_p + b7\Delta T_s + b8 = 0$$

$$b11\Delta T_p^2 + (b12 + b13\Delta T_s)\Delta T_p + b9\Delta T_s^2 + b10\Delta T_s + b14 = 0$$

yields two quadratic equations in two unknowns. The solution to the above equations is acquired by trial and error. Each equation is solved for $\Delta T_p$ and the absolute difference of the two calculated values arbitrarily set not to exceed 1°K. The temperature $\Delta T_p$ is incremented by 0.1°K until the two equations yield the desired 1°K difference or less. Equation (44) is then solved for the other unknown $\Delta T_s$.

## LIST OF REFERENCES


Appleby, J. F. "Special Cases of Simulating the Energy Budget of the Earth/Air Interface," Task 65-0005, Meteorology Dept., U.S. Army Electronic Proving Ground, Ft. Huachuca, Arizona, 1958, 157 pp.

Carslaw, H. S., and Jaeger, J. C. Conduction of Heat in Solids, Clarendon Press, Oxford, 1959, 386 pp.

Cary, J. W. "The Drying of Soil: Thermal Regimes and Ambient Pressures," Agricultural Meteorology, Vol. 4, 1967, pp. 353-365.

Cionco, R. M. "A Mathematical Model for Air Flow in a Vegetative Canopy," Meteorological Research Notes No. 5, Meteorology Department, U.S. Army Electronics Research and Development Activity, Ft. Huachuca, Arizona, 1963, 35 pp.

Conaway, J., and van Bavel, C. H. M. "Evaporation from a Wet Soil Surface Calculated from Radiometrically Determined Surface Temperature," Journal of Applied Meteorology, Vol. 6, 1967, pp. 650-655.

Denmead, O. T., and Shaw, R. H. "Availability of Soil Water to Plants as Affected by Soil Moisture Content and Meteorological Conditions," Journal of Agronomy, Vol. 54, 1962, pp. 385-390.

De Vries, D. A. "A New Stationary Method for Determining Thermal Conductivity of Soil," Journal of Soil Science, Vol. 73, 1952, p. 83.

De Vries, D. A. "On the Cylindrical Probe Method for Measuring Thermal Conductivity with Special References to Soils," Australian Journal of Physics, Vol. 11, 1963a, pp. 255-271.

De Vries, D. A. "Thermal Properties of Soils," Physics of Plant Environment, North Holland Publishing Co., Amsterdam, 1963b, pp. 210-235.

Dryden, P. S. "Direct Fluxometer Measurements of the Evaporation from a Bare Soil," Journal of Applied Meteorology, Vol. 6, 1967, pp. 858-864.

Fritschen, L. J., and van Bavel, C. H. M. "Energy Balance Components of Evaporating Surfaces in Arid Lands," Journal of Geophysical Research, Vol. 67, 1962, pp. 5179-5185.

Fuchs, M., and Tanner, C. B. "Evaporation from a Drying Soil," Journal of Applied Meteorology, Vol. 6, 1967, pp. 852-857.

Gardner, H. R., and Hanks, R. J. "Evaluation of the Evaporation Zone by Measurement of Heat Flux," Soil Science Soc. American Proceedings, Vol. 30, 1966, pp. 425-428.

Halstead, M. H. "A Preliminary Report on the Design of a Computer for Micrometeorology," Journal of Meteorology, Vol. 14, 1957, pp. 308-325.

Jackson, R. D., and Kirkham, D. "Method of Measurement of the Real Thermal Diffusivity in Moist Soil," Soil Science Soc. American Proceedings, Vol. 22, 1958, pp. 479-482.

Lemon, E. R. "The Energy Budget at the Earth's Surface," Production Research Report No. 71, USDA, Agriculture Research Service, 1959, 32 pp.

Lemon, E. R. "The Energy Budget at the Earth's Surface: Comparison of Momentum and Energy Balance Methods of Computing Vertical Transfer Within a Crop," Interim Report, ECOM 2-67I-1, Northeast Branch, Soil and Water Conservation Research Division, USDA, Agriculture Research Service, 1967, 19 pp.

Moench, A. F., and Evans, D. D. "Thermal Conductivity and Diffusivity of Soil Using a Cylindrical Heat Source," Soil Science Soc. American Proceedings, Vol. 34, 1970, pp. 377-381.

Penman, H. L. "Estimating Evapotranspiration," American Geophysical Union Transactions, Vol. 37, 1956, pp. 43-50.

Richards, L. A., Gardner, W. R., and Ogata, G. "Physical Processes Determining Water Loss from Soil," Vol. 20, 1956, pp. 310-314.

Richmeyer, R. D., and Morton, K. W. Difference Methods for Initial-Value Problems. New York Interscience Publishers, 1967, 405 pp.

Sellers, W. D. "Potential Evapotranspiration in Arid Regions," Journal of Applied Meteorology, Vol. 3, 1964, pp. 98-104.

Sellers, W. D. "An Investigation of Heat Transfer from Bare Soils," Final Report, DA-AMC-28-043-65-G-11, The University of Arizona, Institute of Atmospheric Physics, 1965a, 88 pp.

Sellers, W. D. Physical Climatology, The University of Chicago Press, 1965b, 272 pp.

Sellers, W. D., and Hodges, C. N. "The Energy Balance of Non-Uniform Soil Surfaces," Journal of Atmospheric Sciences, Vol. 19, 1962, pp. 482-491.

Soil Conservation Service, Soil Survey IBP, Desert Biome Santa Rita Validation Site, Pima County, Arizona, A Special Report, USDA, Agricultural Experiment Station, The University of Arizona, 1970, 5 pp.

Suomi, V. E., and Tanner, C. B. "Evaporation Estimates from Heat-Budget Measurements over a Field Crop," American Geophysical Union Transactions, Vol. 39, 1958, pp. 298-304.

Tanner, C. B. "Energy Balance Approach to Evapotranspiration from Crops," Soil Science Society of America, Vol. 24, 1960, pp. 1-9.

Tanner, C. B., and Lemon, E. R. "Radiant Energy Utilized in Evapotranspiration," Journal of Agronomy, Vol. 54, 1962, pp. 207-212.

Tanner, C. B., and Pelton, W. L. "Estimates by the Approximate Energy Balance Method of Penman," Journal of Geophysical Research, Vol. 65, 1960, pp. 3391-3413.

Van Bavel, C. H. M. "Surface Energy Balance of Bare Soil as Influenced by Wetting and Drying," Interim Report, 2-67P-2, United States Water Conservation Laboratory, 1967, pp. 1-64.

Van Bavel, C. H. M., Fritschen, L. J., and Reginato, R. J. "Surface Energy Balance in Arid Lands Agriculture: 1960-61," Production Research Report No. 76, USDA, Agricultural Research Service, 1963, 46 pp.

Welely, M. L., Thurtell, G. W., and Tanner, C. B. "Eddy Correlation Measurements of Sensible Heat Flux Near the Earth's Surface," Journal of Applied Meteorology, Vol. 9, 1970, pp. 45-50.

Wiegand, C. L., and Taylor, S. A. "Temperature Depressions and Temperature Distribution in Drying Soil Columns," Soil Science, Vol. 94, 1962, pp. 75-79.

Wiernega, P. J., Nielsen, D. R., and Hagan, R. M. "Thermal Properties of a Soil Based Upon Field and Laboratory Measurements," Soil Science Soc. American Proceedings, Vol. 33, 1969, pp. 354-360.